

MOLECULAR RECONSTRUCTION OF VACUUM GASOILS

Jan J. Verstraete, Nadège Revellin, Hugues Dulot,
and Damien Hudebine

Institut Français du Pétrole - Development Division
PO Box 3, 69390 Vernaison, France

Introduction

In petroleum refining, both the accurate design and the optimization of conversion processes require the development of reliable kinetic models. In order to account for the differences in reactivity of the various species, more rigorous models containing molecule-based reaction pathways are needed. Such models expect a molecular description of the feed, however. Unfortunately, for petroleum cuts boiling above the naphtha range (gasoil, VGO, residue,), a molecular description can no longer be obtained directly from analyses.

To circumvent this lack of molecular information, a detailed description needs to be obtained from more global analyses. This process of approximating the composition in individual components of a feedstock from overall characterization data of the mixture has lately been referred to as "molecular reconstruction". The idea of these molecular reconstruction algorithms is to generate a discrete set of molecules whose properties mimic the properties of the petroleum cut to be represented.

Liguras and Allen¹ proposed to use a predefined set of key components and to numerically adjust their molar fractions in order to obtain a mixture that closely resembles the input analytical data. Unfortunately, this approach is based on an *a priori* definition of the components, while the adjustment of the mixture composition requires a large amount of analytical data, which are not necessarily available to refiners. To overcome these limitations, Neurock et al.² developed a method that was termed "stochastic reconstruction". To arrive at a description on a molecular level, a set of distributions of molecular structural attributes was first defined and then sampled by a Monte Carlo method so as to obtain an equimolar mixture of molecules. When coupled to an optimization loop, the method has been proved able to yield mixtures that closely reproduce the properties of heavy asphaltene fractions³.

During previous work⁴, two different algorithms were developed to generate a complex mixture of molecules from standard petroleum analyses: a stochastic reconstruction technique and a reconstruction method based on information entropy maximization. These algorithms were validated on FCC gasolines and on Light Cycle Oils (LCO)⁵. In the present work, a combination of both approaches will be applied to the molecular reconstruction of vacuum gasoils.

General description of the algorithm

The proposed algorithm consists in two distinct steps. After defining a molecule construction scheme tailored to the specific petroleum cut, a large set of molecules is generated via a stochastic reconstruction method. This generation is iteratively improved until it results in an equimolar mixture whose properties are close to this reference petroleum fraction. This mixture is subsequently used as a starting point and its representativeness is improved by modifying the molar fractions of the various molecules via an information entropy maximization method.

Generation of an initial set of molecules. In the first step, a set of molecules that are typical of the petroleum cut to be represented needs to be created. In this work, a stochastic reconstruction algorithm is used to create a large set of molecules that are assembled from a number of structural attributes (polycyclic

cores, rings, chains, substituents,). In order to create a molecule, the type and number of these attributes are selected by randomly sampling a set of parametric distributions of the building blocks via a Monte Carlo method. During the assembly of the selected structural attributes into a molecule, a "construction scheme" and "building rules" are used to avoid the creation of unfeasible or unlikely molecules. The construction scheme is a decision tree that controls the sequence in which the various attributes are sampled. The building rules are constraints that are used to correctly assemble the various building blocks and to discard unlikely molecules based on thermodynamic or likelihood grounds. The molecule construction procedure is repeated N times in order to obtain an equimolar mixture of N molecules. For each molecule, pure compound properties are calculated from their structure, either directly by inspection (e.g. chemical formula, molecular weight, NMR, mass spectra) or numerically by group contribution methods (e.g. density, boiling point). The average properties of the mixture of N molecules are then obtained through mixing rules and compared to the available analytical data of the petroleum cut (elemental analysis, density, molecular weight, mass spectrometry,). The deviation between the experimental and simulated data is then quantified via an objective function. An elitist genetic algorithm finally modifies the parameters of the distributions for the structural attributes to minimize this objective function (Figure 1). By this procedure, the generated set of molecules is successively modified until a mixture is obtained that mimics the properties of the petroleum fraction to be represented.

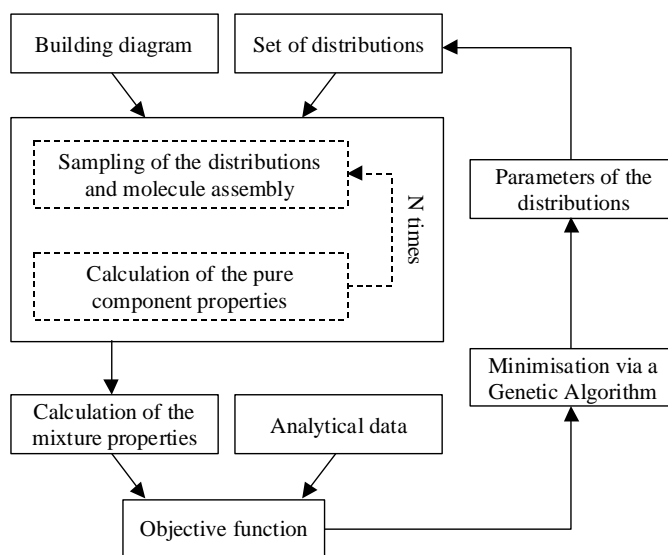


Figure 1. Stochastic reconstruction algorithm.

Enhancement of the molecule-based representation. The initial set of molecules that has been generated by the above described stochastic reconstruction method only yields an average representation of the vacuum gasoil. In order to improve the representativeness of the set of molecules, it is possible to further adjust the molar fractions of these molecules based on the available analytical data. In this work, the adjustment is carried out by maximizing the information entropy. This criterion ensures that, in absence of sufficient information, the distribution of the set of molecules will remain uniform. The introduction of constraints (i.e. analytical data for the petroleum cut to be represented) distorts the uniform distribution of the set in order to match this information. In the current implementation of the algorithm, the only restriction of the method is that the various constraints need to be linear. As

opposed to the stochastic reconstruction technique, the entropy maximization method uses a classical optimization technique. For a more detailed description of the algorithm, the reader is referred to Hudebine et al.⁵.

Application to vacuum gasoils

In order to apply the above-described method to the molecular reconstruction of vacuum gasoils, an adapted molecule construction scheme needs to be defined. This requires detailing, on the one hand, the type and distribution of each structural attribute, and the construction scheme and building rules on the other hand.

The choice of the structural attributes and their distributions has been guided by knowledge of the chemical nature of these cuts, although care has been taken to minimize the number of attributes. For vacuum gasoils, the number of polycyclic cores per molecule was limited to one. The corresponding distribution for this attribute must therefore be a histogram with 2 bins: 0 or 1. Analogously, the number of rings in the polycyclic cores was limited to 7. To reduce the number of parameters, the corresponding distribution is considered to be a gamma distribution. Table 1 lists the distributions used to build a vacuum gasoil.

Table 1. Description of the Structural Attributes Used

Structural attribute	Distribution	Values	Param.
1. Number of polycyclic cores	Histogram	0 or 1	1
2. Number of rings	Gamma	0 .. 7	2
3. Presence of aromatic rings	Histogram	0 or 1	1
4. Number of benzenes	Exponential	0 .. 7	1
5. Number of hetero-atomic rings	Histogram	0, 1 or 2	2
6. Number of thiophenes	Histogram	0 or 1	1
7. Number of pyridines	Histogram	0 or 1	1
8. Number of pyrroles	Histogram	0 or 1	1
9. Alkyl chain probability	Histogram	0 or 1	1
10. Sulfide substituent probability	Histogram	0 or 1	1
11. Amine substituent probability	Histogram	0 or 1	1
12. Length of a paraffin chain	Exponential	> 0	1

The construction scheme allows to define the sequence in which the distributions are sampled. For a given molecule, the number of polycyclic cores is first selected. If this number is equal to 0, the molecule is a paraffin. Distribution 12 is then used to determine its length and each carbon atom is tested to define whether a sulfide or amine substituent should be added (distributions 10 and 11). If the number of cores is equal to 1, distribution 2 gives the total number of rings in the core, while distribution 3 indicates whether aromatic rings are present. In the latter case, the number of benzene rings and the number of hetero-atomic rings are given by distributions 4 and 5 respectively, while the number of naphthenic rings is calculated by difference. The type of the hetero-atomic rings is defined by distributions 6, 7 and 8. Once the various elements are assembled into a polycyclic core, each peripheral carbon atom is tested to check whether an alkyl chain should be inserted or not (distribution 9). The length of the alkyl chains is determined by distribution 12. Finally, distributions 10 and 11 are used to add sulfide and amine substituents.

With this molecular construction scheme, the stochastic reconstruction was used to generate an initial set of 5000 molecules that was obtained after minimization of the objective function. The latter contains the differences between the experimental and calculated values for the elemental analysis, the density, the basic nitrogen content, the liquid chromatography S.A.R. distribution and the detailed Fisher⁶ mass spectrometry analysis. As can be seen in Table 2, the properties of the initial equimolar mixture of molecules obtained at the end of the stochastic reconstruction step are already close to the corresponding experimental values. Some differences

still exist, especially in the simulated distillation curve, which was not included in the objective function, and in the Fisher analysis.

The second step of the algorithm adjusts the molar fractions of the various molecules via an entropy maximization method that minimizes the differences between experimental and calculated values for the simulated distillation curve, the elemental analysis, the basic nitrogen content, the liquid chromatography S.A.R. distribution and the detailed Fisher mass spectrometry analysis. The properties of the resulting final mixture are very close to the corresponding experimental values, indicating that this mixture is a good representation of the actual vacuum gasoil.

Table 2. Comparison of the Properties of the Vacuum Gasoil and of the Corresponding Molecular Set

	Exp.	Initial	Final
Simulated Distillation			
0% (°C)	388	363	363
5% (°C)	426	374	424
10% (°C)	434	388	434
30% (°C)	454	434	455
50% (°C)	476	469	475
70% (°C)	501	511	501
90% (°C)	529	592	528
95% (°C)	536	626	537
100% (°C)	543	-	568
Elemental analysis			
Carbon (wt%)	87.09	87.04	87.10
Hydrogen (wt%)	12.27	12.33	12.28
Sulfur (wt%)	0.47	0.43	0.49
Nitrogen (wt%)	0.17	0.20	0.13
Density at 15°C (g/ml)	0.9247	0.9294	0.9246
Basic nitrogen (wt%)	0.06	0.12	0.04
Liquid chromatography class			
Saturates (wt%)	58.6	59.1	58.6
Aromatics (wt%)	31.6	32.1	31.6
Resins (wt%)	9.8	8.8	9.8
Partial Fisher mass spectrometry			
C _n H _{2n+2} (wt%)	18.0	18.8	18.0
C _n H _{2n} (wt%)	15.2	5.4	15.2
C _n H _{2n-2} (wt%)	29.3	8.6	29.3
C _n H _{2n-4} (wt%)	0.0	7.1	0.0
C _n H _{2n-6} (wt%)	4.6	7.5	4.6

Conclusions

A molecular reconstruction algorithm was developed for vacuum gasoils. The proposed two-step algorithm first generates an initial equimolar set containing a large number of molecules via a stochastic reconstruction method. The representativeness of this mixture is subsequently refined by modifying the molar fractions of the various molecules via an information entropy maximization method. The properties of the resulting set of molecules are very close to vacuum gasoil to be represented, indicating that this mixture can now be used as input to a detailed reaction scheme for hydrocarbon conversion processes.

Acknowledgements. The authors wish to acknowledge G. Bailleux for his contribution to this work.

References

- (1) Liguras, D.K.; and Allen, D.T.; *Ind. Eng. Chem. Res.*, **1989**, 28 (6), 674-683
- (2) Neurock, M.; Nigam, A.; Trauth, D.; and Klein, M.T.; *Chem. Eng. Sci.*, **1994**, 49 (24A), 4153-4177
- (3) Trauth, D.M.; Stark, S.M.; Petti, T.F.; Neurock, M.; and Klein, M.T.; *Energy & Fuels*, **1994**, 8 (3), 576-580
- (4) Hudebine, D.; Ph.D. thesis, Ecole Normale Supérieure - Lyon, **2003**
- (5) Hudebine, D.; Vera, C.; Wahl, F.; and Verstraete, J.J.; 2002 AIChE Spring Meeting, New Orleans, LA, March, 10 - 14
- (6) Fisher, I.P.; and Fischer, P.; *Talanta*, **1974**, 21, 867-874

CHARACTERIZATION OF ASPHALTENES FROM MARLIM VACUUM RESIDUE USING HEPTANE TOLUENE MIXTURE

B.Avid, S. Sato, T. Takanohashi, I.Saito

Institute of Energy Utilization, National Institute of Advanced Industrial Science, 16-1 Onogawa, Tsukuba 305-8569, Japan

Introduction

Thermal cracking processes are commonly used today to convert petroleum vacuum residue (VR) into distillable liquid products. Petroleum asphaltene (AS), the heaviest, most aromatic component of crude oil, tend to precipitate to cause coking during thermal and catalytic processing of petroleum residues. Except of the temperatures and residence times of the cracking, a number of factors are important during coking such as, the asphaltene concentrations in the feed, molecular weight, structure, aromaticity, metal and heteroatom content of the asphaltenes and nature of solvent [1-4]. The objective of this process is to maximize the yield of cracked products, on the other hand, to avoid the formation of coke deposits. These goals are only achievable through a better understanding of mechanism of the process and asphaltene structure. It is well recognized that asphaltenes from different crude oil sources can have vastly different properties. For example, two types of asphaltenes exist in the Athabasca bitumen- one type tending to lower molecular weight and having a few condensed aromatic rings per unit and the other type having a higher molecular weight and considerably more (up to c.30) condensed aromatic rings per unit [5]. Rahimi pointed out that only a portion of the asphaltenes converted to coke while the remaining portion converted to maltenes and gases [1]. Most of these studies have been concerned with simplified systems, in which asphaltenes had been extracted from their natural medium by precipitation in an excess of n-heptane (or n-pentane) and then redissolved in different solvents or re-mixing with VR to characterize the asphaltene structure, molecular size, coke formation, aggregation and so on. Despite of these efforts, there are currently not clear picture of the asphaltene structure, conversion and mechanism of thermolysis.

The objective of this work was to separate the Marlum VR by using n-heptane-toluene mixtures and examine the behavior of the separated fractions in the coking test. The elemental analysis, NMR and GPC were applied to characterize the separated asphaltenes.

Table 1. Properties of Marlum Vacuum Residue

Elemental analysis	
C, wt %	87.2
H, wt %	10.6
N, wt %	0.69
S, wt %	0.98
O, wt %, by diff.	0.53
H/C ratio	1.45
V, ppm	73
Ni, ppm	59
fa	0.29
Molecular weight	935
Asphaltene, wt %	13.3

Experimental

The VR from Marlum crude oil (Brazil) has been used in this experiment (Table 1). The asphaltenes were precipitated from VR using n-heptane-toluene mixture (heptol), and soluble part, i.e. maltene (MA) was recovered from heptol. The content of toluene in the mixture was ranged from 0 % to 60% (by volume) and separated products were named as AS0%-AS60% and MA0%-MA60%, respectively. All samples were analysed by NMR, GPC and elemental analyses.

NMR analysis was carried out by a JEOL Lambda 500 spectrometer by applying inverse gated decoupling and DEPT pulse sequence of 45° and 135°. The distribution of aliphatic CH₃, CH₂ and CH and quaternary aromatic carbon were determined by ¹³C-NMR and DEPT techniques [6-8].

Average molecular weight was measured by GPC system (JASCO) using KF403HQ Shodex column (exclusive limit 70,000) and Evaporative Laser Scattering Detector (ELSD) with chloroform as an eluent and polyethylene as calibration standard for molecular weight. Experiments for coke formation were carried out batchwise in an 18 ml quartz tube. The tube was loaded with 3 g of reactant and placed in a 50 ml metal reactor and pressurized with nitrogen at 1 MPa. The reactor was heated in an agitated oven at 430 °C for 1 hour and cooled to room temperature. Then reactor was vented and gas was analysed by GC, liquid product was washed by toluene and kept overnight.

The toluene insoluble product (coke) was separated by centrifuge and cake was washed again by toluene. Toluene was removed from the filtrate by rotary evaporation followed by vacuum drying at 60 °C overnight to give the coke yield.

Results and discussion

The Marlum VR was separated into the asphaltene (AS) and maltene (MA) fractions by heptol. In the case of 60% heptol, the VR was completely dissolved (no precipitation), meanwhile yield of AS 40 % was negligible, and therefore the separated products from 0 to 30 % heptol were used in further investigations. The Marlum VR and different maltene fractions (MA0%-MA30%) were examined by coking test and results of these shown in Fig.1.

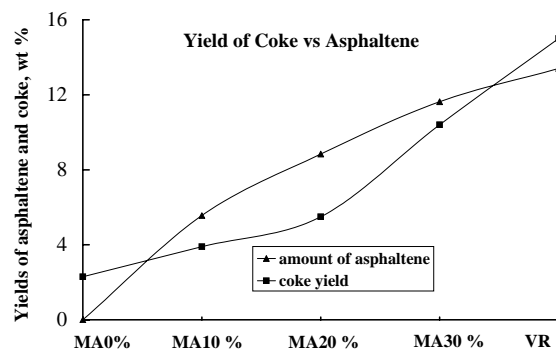


Fig.1. The correlation between coke and asphaltene

The purpose of the experiment was just to examine the conversion of different asphaltene fractions into coke under normal processing condition. Coke is defined as insoluble in an aromatic solvent such as benzene or toluene. As mentioned before, the high content of asphaltene in vacuum residues tends to give high yield of coke. As

shown in Fig. 1, the yield of the coke was increased by 2.2 wt% with increasing of asphaltene by 9.3 wt% in the MA0% to MA 20%. The influence of asphaltene for the coke formation was negligible. But from the MA20% to MA30 %, yield of the coke was increased obviously, i.e. coke yield was raised from 5.5 to 10.5 wt%, even the content of asphaltene increased just by 3.1 wt% in this range. In this case, the increment of coke was two times higher than asphaltene increment. As can be seen from the results obtained in this work, the asphaltene exerts differently for the coke formation due to asphaltene properties. i.e. asphaltenes in the MA0%-MA30% fractions were not same, or according to Rahimi [1], the portions of asphaltenes, which are converted into the coke or maltene were significantly different in the fractions. By the other hand, portion of asphaltenes converts into maltene or gas was higher in the AS of the MA10% and MA20 % than in the MA 30%, or portion of asphaltene converts into coke was higher in the MA30%. In order to clarify the properties of different asphaltene fractions, Marlim VR asphaltene was separated into AS 0-10%, AS10-20%, AS 20-30% and AS 30 % and these fractions were analysed by elemental analysis, NMR (Fig.2) and GPC (Table 2).

The elemental analyses of the separated AS were similar, except hydrogen content. The hydrogen content of fractions is decreasing from AS0-10 % to AS30 %, and as well AS0-10% and AS10-20 % have a higher H/C ratio than AS20-30% and AS30 %. Average molecular weights (Mn) of the AS are in the range of 690 to 810 daltons. Also there is a little increase of Mn from AS0-10 % to AS20-30%. But the difference is not so high. The ¹H NMR analysis shows a similar distribution of the different asphaltene fractions. The aromatic proton content (Ha) is around 11%. The aromaticity (fa) is increasing from fraction AS0-10% to AS30 %, i.e. AS20-30% and AS30 % have a higher fa (0.53) than first 2 fractions and total AS (0.48). The AS20-30 % and AS30% had the highest percentage of quaternary aromatic carbon (QAC), which are equal to around 40 wt% and AS 0-10% and AS10- 20% had a lower QAC (35-37 wt%). The distribution of non aromatic carbons shows that fraction of CH is decreasing from AS0-10% to AS30 %, the distribution of CH₂ was opposite, i.e. increasing in this range. It is likely that the AS, which have a higher aromaticity and quaternary aromatic carbon, produces more coke than AS with lower fa and QAC. Therefore, AS 0-10% and AS10-20 % were named as GOOD AS and AS20-30% and AS30 % are BAD AS.

Conclusions

The Marlim VR was separated into asphaltene (AS) and maltene (MA) fractions using n-heptane-toluene mixtures and separated MA fractions examined for coking test and results show that the AS is consisted of BAD AS and GOOD AS. So the asphaltene were fractioned into AS 0-10%, AS10-20%, AS 20-30% and AS 30 %. The AS 20-30% and AS30% have a higher aromaticity and quaternary carbons and produce more coke than the AS 0-10% and AS10-20%.

Acknowledgements

B.A. would like to thank for the JSPS fellowship. Also we are grateful to Dr. Y.Sugimoto, M. Kouzu and Mr. H. Ozawa (AIIST) for help on using apparatus for coke experiments.

References

- Rahimi P., Gentzis T., Taylor E., Carson D., Nowlan V., Cotte E., *Fuel*, **2001**, 80, 1147-54
- Rahmani S., Mccaffrey W., Gray M.R., *Energy & Fuel*, **2002**, 16, 148-154
- Groenzin H., Mullins O.C., *Journal of Phys. Chem. A*, **1999**, 103, 11237-45

- Rahmani S., Mccaffrey W., Dettman H., Gray M.R., *Energy & Fuel*, **2003**, 17, 1048-56
- Mitchell, D.L. and Speight, J.G. *Fuel*, **1973**, 52, 149-152
- Netzel, D., *Anal. Chem.*, **1987**, 59, 1775- 1779
- Kotlyar, L.S., Morat, C. and Ripmeester, J.A., *Fuel*, **1991**, 70, 90-94
- Masuda K., Okuma O., Nishizawa T., Kanaji M. and Matsumura T., *Fuel*, **1996**, 75 (3), 295-299

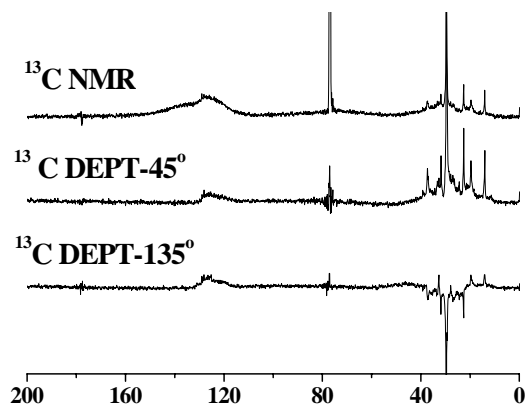


Fig.2. Typical NMR spectra of the asphaltene fractions

Table 2. Properties of the Marlim VR Asphaltenes

Sample name	Total AS	AS0-10%	AS10-20%	AS 20-30%	AS 30%
Recovery, wt%	14.2	4.1	4.7	3.6	1.8
Elemental analysis, wt%					
C	86.2	85.9	86.5	87.3	85.8
H	8.01	8.40	8.27	8.11	8.01
N	1.28	1.25	1.29	1.32	1.19
S	1.27	1.27	1.21	1.21	1.24
O	3.24	3.22	2.73	2.06	3.76
H/C	1.11	1.17	1.14	1.11	1.11
Mn (GPC)	691	743	748	806	758
NMR analysis, %					
¹H-NMR					
Ha	10.5	11.1	11.4	12.4	11.1
H α	16.7	15.7	16.7	16.5	16.3
H β	51.6	56.8	56.2	53.0	52.7
H γ	21.2	16.3	15.6	18.1	19.9
¹³C-NMR					
fa	0.48	0.49	0.50	0.53	0.53
QAC	34.9	36.2	37.4	39.1	40.5
Distribution of non-aromatic carbons					
CH	20.53	15.90	15.89	13.57	10.09
CH ₂	61.24	64.39	64.85	67.43	70.56
CH ₃	18.23	19.71	19.26	19.00	19.35

QAC- Quaternary aromatic carbon

Heavy product from co-processing of FCC slurry and coal as bitumen modifier

Yongbing Xue, Jianli Yang*, Zhenyu Liu, Zhiyu Wang, Zenghou Liu, Yunmei Li and Yuzhen Zhang**

State Key Laboratory of Coal Conversion
Institute of Coal Chemistry, Chinese Academy of Sciences
Taiyuan 030001, P.R.China

** Institute of Heavy Oil Research, Petroleum University
(Dongying)
Dongying 257061, P.R.China

Introduction

Co-processing of coal and petroleum resid has been developed to produce liquid fuels, and has gained significant advancements during past several decades. In this work the co-processing process is adopted to produce a bitumen modifier under mild conditions. The modifier is the heavy portion of the co-processing products including un-reacted materials and ash in the coal. Oil is a byproduct. Market price of similar natural occurring modifier is about \$500-\$750/t in China, which is much higher than the prices of oil and road paving asphalt.

Bitumen on road experiences a wide range of static and dynamic stress at varying temperature under different environmental conditions. The lifetime of the road surface is limited due to aging of bitumen in asphalt concrete mix. Addition of non-vulcanized nature and synthetic polymers to improve the properties of paving asphalt are well known and widely used (1, 2). Reclaimed rubber, pulverized waste tire and special naturally occurring asphalt (such as Trinidad lake asphalt) are also used as additives (3, 4). Addition of these materials improves durability of asphalt surface, adhesion of bitumen to aggregate, deformation resistant at great load and freeze resistance.

Due to super road performance (4), compared to other additives, Trinidad lake asphalt (TLA) has been used in bitumen modification worldwide.

In this study slurry, from fluidized catalytic cracking (FCC) unit, and coal is co-processed. The heavy product, named MCSC (modifier from co-processing slurry and coal), is tested for possible usage on bitumen modification. Modification ability and physical and chemical properties of MCSC are presented and compared with TLA.

Experimental

The FCC slurry (FCCS), from Shijiazhuang Petroleum Refinery of China, and a Chinese bituminous coal (YZ), were used to make the modifier, MCSC. The properties of FCCS and the coal are listed in Tables 1 and 2. The base bitumen used to test the modification ability of the modifier was Binzhou 90# (AH 90 in Chinese standard specification) with a penetration value of 95. The base asphalt was mixed mechanically with the modifier.

The co-processing was carried out in a 50-liter autoclave with a magnetic stirrer under hydrogen or nitrogen pressures of 8-14 MPa at temperatures of 400-450°C for 1-3 hours. The coal was pulverized to <100 mesh and impregnated with a Fe (1 wt%) or a Mo (0.04-0.4 wt%) catalyst precursor (5). The ratios of FCCS to coal were 1:1 and 2:1. The autoclave was directly connected to a 40-liter vacuum distillation unit. After the co-processing, the mixture was discharged into the distillation unit and the oils were distilled out at 330°C and 0.01MPa. The residual materials were MCSC and collected from the

bottom of the distillation column. Typically the MCSC yield ranged from 65-80% and oil yield 10-25% (boiling point ranged from 100-450°C).

The Technical Specifications of JTJ 036-98 for Construction of Highway Modified asphalt Pavement, and standard test methods JTJ 052-2000 for Bitumen and Bituminous Mixtures of Highway Engineering by Ministry of Communications of The People's Republic of China, were used.

Table 1. The Properties of the FCCS Used, wt% as¹

Elemental composition				
C	H	N	S	H/C, atomic
88.97	8.12	0.48	1.35	1.1
Group composition				
Saturates	Aromatics	Resins	Asphaltenes	
6.7	65.7	18.7	8.9	

1: "as" denotes "as received"

Table 2. The Properties of the Coal, wt% as¹

Proximate analysis				
Moisture	Ash	Volatile Matter		
1.50	4.17	42.86		
Ultimate analysis				
C	H	N	S	H/C, atomic
75.92	5.01	1.32	2.02	0.79

1: "as" denotes "as received"

Results and Discussion

The properties of a typical MCSC and TLA are compared in Table 3. There is no significant difference in physical properties listed in the first five lines. The main differences are in the last two lines, which reveal the higher aromaticity of MCSC than TLA, the lower hydrogen content and the higher aromatic hydrogen distribution in MCSC. The high contents of organic residue and pre-asphaltene are significant factors, which differentiate MCSC from TLA.

Comparisons of modification abilities of MCSC and TLA are given in Tables 4 and 5. The mixing ratio of the modifier to the base bitumen is 20:80. The notation 90#/MCSC refers to a modified Binzhou 90# by MCSC, 90#/TLA refers to a modified Binzhou 90# by TLA. From Table 4 it can be seen that both MCSC and TLA alter the properties of the base bitumen, increasing the softening point by about 4-8°C and decreasing the penetration value by about 51-54 points. This indicates that the modified bitumen becomes harder than the base bitumen. Usually, this change may result in loss of viscoelasticity to some extent. But the data show that the viscoelasticity of the modified bitumen samples is still very good as demonstrated by the high ductility values at 15°C and 25°C. The Retained penetration (the ratio of penetration value after and before TFOT, thin-film oven test, which represents the ability on resisting the fast aging) of both modified samples are also higher, suggesting higher high-temperature stability. The ductility of 101 mm for 90#/MCSC at 15°C suggests higher low-temperature stability of the sample. All these data suggest that the properties of 90#/MCSC are significantly better than that of 90#/TLA.

Table 5 compares dynamic stabilities between 90#/MCSC and 90#/TLA samples determined in the rutting test. Rutting is generated at a wheel path of carriageway in the cases of warmer climate

* Corresponding author. Tel/Fax: +86-351-404-8571
E-mail address: jyang@sxicc.ac.cn

conditions, heavily trafficked roads, approaches to intersections and climbing lanes. Dynamic stability of hot mix asphalt (HMA) against rutting is an important property of asphalt mixture in wearing course. It represents the ability to resist showing rutting under traffic and elevated temperature. For hot mix modified bitumen mixture this value should be greater than 800-3000 wheel passes/mm depending on the climate encountered. It is clear that the dynamic stabilities of both samples are similar and meet the highest required value.

Table 3. The Properties of Typical MCSC and TLA

Items	MCSC	TLA
Specific gravity	1.15	1.39-1.44
Softening point (R&B), °C	102	93-99
Penetration at 25°C, 100g, 5s	8	0-4
Weight loss after thin-film oven test, %	<1	<2
Solubility in trichloroethylene, %	53	52-55
Inorganic residue, %	3	35-39
Organic residue, %	20	8
Preasphaltene, %	33	0.73
THF solubles, %	75	56
H/C, atomic	0.8	1.4
Aromatic/aliphatic hydrogen ratio by FTIR	7.4	0

Table 4. The Properties of Binzhou 90# and Two Modified Bitumen

Items	90#	90# /MCSC	90# /TLA
Softening Point (B&R), °C	44.2	48.0	51.7
Penetration at 25°C, 100g, 5s	95	44	41
Ductility at 25 °C , 5cm/min, cm	>150	>150	>150
Ductility at 15 °C , 5cm/min, cm	>150	101	52
Flash point, °C	>240	>240	>240
TFOT			
Softening Point (B&R), °C	48.7	53.6	56.1
Penetration at 25°C, 100g, 5s	57	36	26
Retained penetration after thin-film oven test, %	60	82	63
Ductility at 25°C, 5cm/min, cm after thin-film oven test	150	144	100
Weight lost, %	0.100	0.255	0.418

Table 5. The Results of the Rutting Test

Sample	90#/MCSC	90#/TLA
Dynamic stability, wheel passes/mm (60°C, 0.7 MPa)	2000-3500	3100

Further comparison on the properties of 90#/MCSC and 90#/TLA samples with ASTM standard specification, D5710-95, designated to Trinidad lake modified asphalt, showed that both modified samples meet the specifications.

It was also found that the properties of the modifier are related on the co-processing conditions used, such as temperature, atmosphere, pressure, type of catalyst, catalyst loading, FCCS to coal ratio and reaction time. Two or more modifiers can also be blended to obtain the desired properties. The properties of the modifier can be manipulated by controlling the co-processing conditions.

Conclusions

A heavy product (MCSC) produced from co-processing of a fluidized catalytic cracking slurry with a coal was used as bitumen modifier in asphalt concrete mix. The modification capability of MCSC is similar to that of a commercial bitumen modifier, Trinidad lake asphalt (TLA), and meets ASTM standard specification of D5710-95. Comparing to TLA, MCSC contains more aromatic, condensed, small molecular weight component.

Acknowledgement.

The Natural Sciences Foundation of China (20076050, 20076049) and Chinese Academy of Sciences are acknowledged for the financial supports. Chief Engineer Yanti Wang of Shijiazhuang Petroleum Refinery, Director Zhe Wang of Shanxi Provincial Communications Planning Survey and Design Institute, Chief Manager Zhigang Ye of Shandong SHTAR Science and Technology, Professor Bijiang Zhang of Institute of Coal Chemistry, and Manager Wen Zhou of department of bitumen of Sino Fame LTD. are also acknowledged for their valuable suggestions and providing FCCS and asphalt samples. The project is also partially supported by the Special Funds for Major State Basic Research Project (G19990221).

References

- (1) Yang, Z.; Cheng, G. *Petroleum Asphalt*, **2001**, *15*, 1
- (2) Xue Y.; Yang, J.; Liu, Z. *Highway* **2001**, *11*, 120
- (3) Ye, Z.; Kong, X., Yu J.; Wei Q.; Jiang, Z *Journal of Wuhan University of Technology*, **2003**, *25*, 11
- (4) Shen, J.; *Journal of Foreign highway*, **2000**, *20*, 28
- (5) Yang, J.; Zhu, J.; Xu, L.; Liu, Z.; Li, Y.; Li, B. *Fuel*, **2002**, *81*, 1485

CHARACTERIZATION AND CRACKING PERFORMANCE OF THE MODIFIED USY ZEOLITES WITH MIXED ORGANIC ACID

Chunmin Song and Zifeng Yan

Chemistry Division
State Key Laboratory for Heavy Oil Processing
University of Petroleum
No. 271, Bei'er Road
Dongying, China, 257061

Introduction

Fluid catalytic cracking (FCC) is one of the most important refining processes, and plays a key role in whole petroleum refining industry. 70-80% gasoline, 30-40% diesel oil and 50% propylene is come from catalytic cracking units, especially in China. Industrially, cracking reaction of hydrocarbons is catalyzed by the acid-form zeolite, especially by Ultrastable Y zeolites, which were prepared by steam dealumination of Y zeolite at high temperatures.¹ The distribution of the cracking products depends on the performance of zeolites and the reaction conditions. Hence the nature of acid sites of zeolites may strongly influence the performance of the catalytic cracking of hydrocarbon. Therefore many researchers have attempted to modify or post-synthesize zeolites to obtain optimum number and strength of acid sites and suitable pore structure with high activity and given selectivity. In addition, with the feedstocks of FCC being heavier and poorer and the tendency of increasing lighter olefins and diesel, the features of the mesopores and acid sites of USY zeolites will not meet the variation of materials in the future. Thus the modification of USY zeolite have been further paid much attention.²

There are different ways to modify the Y zeolite, such as hydrothermal treatment, vapor phase substitute dealumination of the high temperature, post-synthesis using $(\text{NH}_4)_2\text{SiF}_6$ and extraction by acid complexation.³ Here the USY zeolites were treated with tartaric acid and citric acid in unbuffered system. In this process, the skeletal aluminum atom might be coordinately extruded by complex form from the skeleton of zeolite. Furthermore, the crystal structure, physical adsorption property, stability, catalytic cracking property of the modified zeolites were investigated by XRD, N_2 adsorption, FT-IR and micro-activity test (MAT). The nanopore volume, distribution and cracking Performance of the modified USY zeolites were extensively investigated in this paper.

Experimental

Preparation of modified USY zeolites. The USY parent zeolite supplied by Lanzhou Work of catalyst, whereas USY is already in its hydronium form, in which Si/Al ratio is 11.8 and the unit cell constant is 2.4432 nm. The process as follows: 6 gram of USY zeolite was placed into a three-necked flask with a certain amount dilute nitric acid as the solvent and this mixture was stirred and heated to 90°C. Then the mixed tartaric acid and citric acid solution was added. The solution was stirred for 4 h at 90°C. After reaction, the gel was filtered, washed, and dried overnight at 120°C.

Characterization Methods. The crystal structure parameter of samples was measured by X-ray diffraction (XRD) technique with a Rigaku D/max-III A X-ray diffractometer using $\text{Cu K}\alpha$ radiation. N_2 adsorptions for the samples were carried out on a Micromeritics ASAP-2010 instrument using nitrogen as adsorbate at 77K. Before adsorption measurements the samples were degassed for 4 h at 673K. The mesopore size data were analyzed by the BJH method. The micropore size distribution was obtained by H-K method.

Micro-activity test (MAT). The modified sample was powdered, and mixed with kaolin clay matrix in the proportion of 30:70 wt% to prepare modified zeolite catalyst, while the diameter of catalyst particle is about 100-150 mesh. The catalyst was treated at 800°C with 100% steam for 4 hours prior to catalytic reaction. The catalytic cracking activity of the catalyst was assessed with an MRCS-8006 type microreactor, which is designed according to ASTM D-3907-80. The feedstock is Shenghua VGO, supplied by Shenghua Oil Refinery Factory, University of Petroleum. The density of feedstock is 0.8857 g/cm^3 (20°C). Reaction temperature was 550°C and the ratio of catalyst to oil was 3. The liquid products were analyzed by HP5880A chromatography of simulating distillation. The vapor products were analyzed by HP5890 II GC equipped with a FID and a 50m fused silicon capillary column. The reacted catalyst were analyzed by self-made carbon mensuration, and worked out coke content of catalyst. The amount of gasoline and of diesel was calculated by simulating distillation. The distillates <204°C was distributed to gasoline part, and between 205 and 350°C was assigned as diesel part, and >350°C referred to heavy oil part, which might be assigned as the not converted feed part.

Results and Discussion

USY zeolite is typical active component for hydrocarbon cracking catalysts, which has special nanopore and acid sites. The special nanopores insure the product selectivity and acid sites hold out the high conversion of heavy hydrocarbons. It means that optimization of nanopore and acid sites of zeolites might be the key to design the effective catalyst of hydrocarbons cracking. The current USY zeolites that has been employed industrially is obtained by hydrothermal dealumination under high temperature. Its dealumination degree is rather limited, and that the non-framework aluminum formed during the steam treatment may affect the catalytic performance of zeolites catalysts. Here USY zeolites were modified with tartaric and citric acid in unbuffered system. The modification results indicate that modified zeolite samples with higher Si/Al ratio can be prepared by this method, which shows higher yields of lighter olefin and diesel oil in traditional FCC process. The investigation indicates that the PH value and the amount of the tartaric and citric acid have greatly influence, and that the treatment time and the drop velocity of the acids has little influence on the modification.

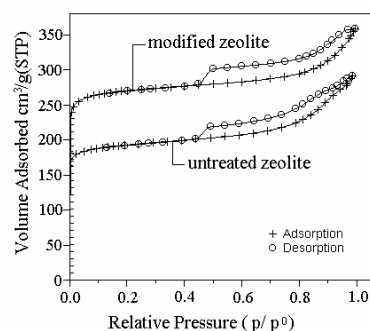


Figure 1. Nitrogen adsorption isotherms of untreated zeolite and modified zeolite.

The results of XRD patterns show that the Si/Al ratio of modified samples increases as compare to that the parent zeolite. This indicates that chemical dealumination of USY zeolite result in framework reconstruction of USY zeolite skeleton. Aluminum is subsequently removed from the zeolite crystal as a soluble tartaric and citric aluminum complex. Simultaneously, some extraframework silica fills the skeleton vacancies left by dealumination. Thus, the

structure differences exist between USY and modified samples due to framework dealumination and formation of mesopores.

The isotherms of nitrogen adsorption shown in **Figure 1** indicate that this is in good agreement with the reported in the literature⁴, which attribute to type IV with a distinct hysteresis loop. Furthermore, the nitrogen adsorption amount of the modified samples is increased, but the shape of the isotherm is not change. The micropore distribution of modified samples shown in **Figure 2** indicates that the number of micropore is increased. It means that the pore volume of modified samples is rather more developed than that of the untreated zeolite and the pore distribution gradient is not obviously changed. The increase of micropore may be beneficial not only to the rebuilding of the framework, which leads to the transformation of larger mesopores into several micropores, but also to the enlarging tendency of the existing micropores. Micropore is the major nanopore in modified zeolite. However, it might be favor the deep cracking reactions to produce much more LPG or lighter olefins due to micropore volume increasing.

The mesopore distribution of modified zeolite and untreated zeolite is shown in **Figure 3**. It indicate that secondary mesopore volume is positively improved, and the secondary mesopore diameters of modified samples were concentrated at ca. 3.8 nm, which might be desirable for FCC processes of residual oil or heavy feedstocks. Furthermore, it is also advantage for production of diesel fraction in FCC process.

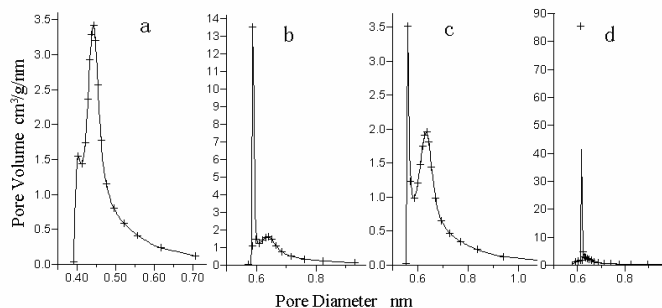


Figure 2. The micropore distribution of modified zeolites (where a is untreated zeolite; b, c and d are modified zeolites).

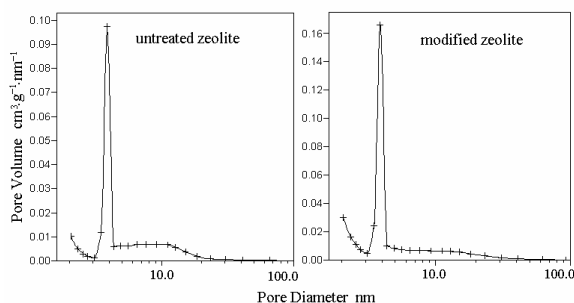


Figure 3. The mesopore distribution of modified zeolite and untreated zeolite

The IR spectra show that the hydroxyls with IR bands of 3610 and 3575 cm^{-1} in the micropores or small cages bears the stronger acidity and much more sites than those in mesopore or larger cavities. The special acid distribution is rather preferable to produce more diesel oil and lighter olefins in FCC process. The catalytic performance of the modified zeolite catalyst is shown in **Figure 4** and **Figure 5**. The result indicates that the diesel yields of the modified samples are effectively improved, and the activity of the

modified catalyst have slightly decreased. Simultaneously, the coke formation of the modified samples were obviously inhibited, and the yield of lighter olefins have partially increased. This is due to the acid sites of the modified samples decrease in number, but enhance in strength. Generally, the lighter olefins should be preferably produced on stronger acid sites in micropores or small cavity, while the diesel distillate is mainly formed on the medium and weaker of acid sites in mesopores or supercages. The modified zeolites have the gradient distribution of acid sites and nanopores. The gradient distribution of acid sites in mesopores or large cavity might effectively inhibits the occurrence of the hydrogen transfer reaction and deep cracking and coke formation, which result in the increase of the yield of lighter olefin and diesel, decrease of the coke yield. Furthermore, the result of the fixed bed evaluation using amplificatory modified samples is in good agreement with that of laboratory test (MAT). Thus optimization of nanopores and acid sites of USY modified with tartaric acid and citric acid in unbuffered system might result in an industrial process to design novel FCC catalysts.

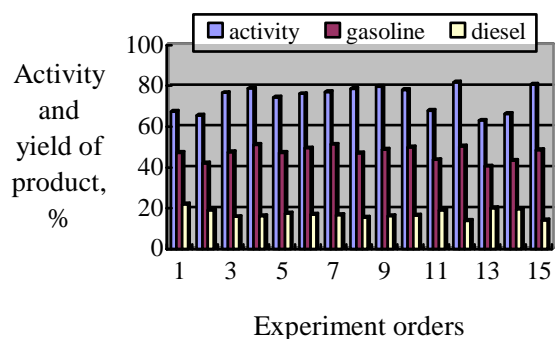


Figure 4. The activity and the yield of gasoline and diesel (where 15 is untreated sample).

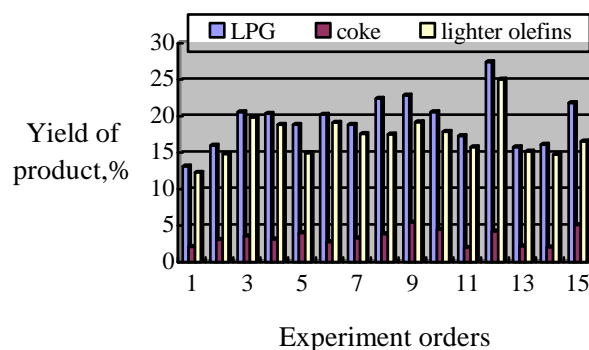


Figure 5. Profile of the product yield (where 15 is untreated sample).

Acknowledgments

We gratefully acknowledge financial support by PetroChina Company Limited (Grant No. 010301-04).

References

1. Fleisch, T.H., Meyers, B.L., Ray, G. J., Hall, J. B., Marshall, C. L., *J. Catal.*, **1986**, 99, 11.
2. Zhou, P., *Petrol. Proc. Petrochem. (China)*. **1997**, 28, 52.
3. Liu, X. M.; Qian, L.; Yan, Z. F., *J. Petrochem. Univ. (China)*, **1997**, 10, 4-26.
4. Nguyen, C., Sonwane, C.G., *Langmuir*, **1998**, 14, 4950

HYDROISOMERIZATION OF N-TETRADECANE OVER P MODIFIED Pt/SAPO-11 CATALYST

Cheng-Hui Geng, Fei Zhang, Zhi-Xian Gao*, Jing-Lai Zhou

Institute of Coal Chemistry, Chinese Academy of Sciences
Taiyuan 030001, P. R. China

Introduction

As is well known, the hydroisomerization process uses a metal/acid zeolite catalyst that has been described as bifunctional¹. Noble metal such as Pt, Pd, and bimetal supported on ZSM-12, mordenite, USY, L-zeolite and β -zeolite have been employed as the bifunctional catalysts for hydrocarbon hydroisomerization process². With these classical catalysts, high isomerization selectivity has been obtained only at relatively low conversion levels, but the selectivity decreases drastically at higher conversion levels and thus the formation of cracking products predominates.

Recently, great improvements have been achieved by using SAPO-11 supported Pd or Pt catalysts^{3,4,5,6,7}. Generally SAPO-11 has a lower acidity than zeolites⁸, and has been proved to more suitable for constituting catalysts that manifest better performance for long-chain hydrocarbon isomerization. The aim of this work is to investigate the effect of the phosphor modification of SAPO-11 on the catalytic activity, product selectivities and time-on-stream stability. The effects of reaction conditions on the catalytic performance were tested by varying reaction parameters such as temperature, pressure and WHSV, as well as the H₂/CH (H₂ to hydrocarbon) ratio. The obtained data were compared with our previous findings and used to interpret the formation of feed isomers as well as their distributions.

Experimental

Catalyst. The calcined SAPO-11 sample was mixed with a certain amount of alumina, and extruded into cylindrical shape. After drying at 120 °C, the extrudate was crushed and sieved to obtain particles with a diameter of about 0.5mm. For P modification, the particle was impregnated with a dilute orthophosphoric acid, followed by drying and calcination at 120 °C and 500 °C, respectively. The amount of P in the sample was designed to be 1% by weight.

SAPO-11 supported Pt catalysts were prepared by incipient wetness method. The obtained samples containing 0.4% platinum are denoted as 0.4Pt/SAPO-11 for non-modified and 0.4Pt/SAPO-11(P) for P-modified samples, respectively. The acidity of support was measured by NH₃-TPD, and the dispersion of Pt was estimated by H₂ chemisorption measurement at room temperature on a self-equipped apparatus system. Details on these characterizations can be found elsewhere⁹.

Catalytic activity measurements. Hydroconversions of *n*-tetradecane were carried out in a 10ml fixed bed reactor system. Previous to activity measurements, the catalyst was pretreated in-situ first with air, then with H₂ up to 400 °C for 2h. Reaction products were analyzed in a GC with a flame-ionization detector. Product identification was achieved by GC-MS and by comparing the retention time of some pure compounds with separate GC injections. The carbon numbers of all the peaks were settled, but only some of the structures could be identified.

Results and Discussion

The hydroconversion of *n*-tetradecane on the two Pt/SAPO-11 catalysts gave both isomerization and cracking products, but with a higher selectivity to feed isomers at low temperatures. The cracking products consisted of spectra of C₁-C₁₃ hydrocarbons with pretty high

percentage of C₃-C₇. Minor amount of C₁ and C₂ were obtained, which suggests that the hydrogenolysis on the Pt/SAPO-11 catalysts of 0.4 metal loading is negligible.

As was expected, the conversion of *n*-tetradecane increased with reaction temperature, while the selectivity to tetradecane isomers decreased gradually. At higher temperatures, with conversion level reaching more than 90%, the cracking reactions became pronounced, giving an isomerization selectivity of less than 10%. As shown in **Fig1**, both the activity and isomerization selectivity are improved by P modification, especially at low temperature range. This may be attributed to the increase of weak acidity by P modification as indicated by NH₃-TPD data.

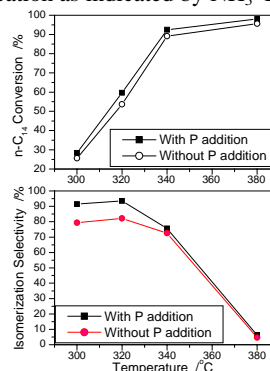


Fig1. Effect of reaction temperature on the hydroconversion of *n*-C₁₄ over 0.4Pt/SAPO-11(P) and 0.4Pt/SAPO-11 catalysts
Condition: P=30atm, WHSV=2.0h⁻¹, H₂/C₁₄=8.7(mol/mol).

Comparing these results with our previous findings¹⁰, which shown more than 80% isomerization selectivity of even at 90% conversion over a SAPO-11 catalyst of the same metal loading, we come to the conclusion that the catalytic behavior is largely influenced by the nature of SAPO-11 molecular sieve.

The effect of total reaction pressure on *n*-C₁₄ hydroconversion was investigated, and the results are presented in **Table1**. As shown in the table, both the conversion of *n*-C₁₄ and the yield of feed isomers decrease with increasing pressure. The results indicate a negative reaction order with respect to hydrogen, which is consistent with the known data^{11,12}.

Table1. Effect of Pressure on *N*-C₁₄ Hydroconversion over 0.4Pt/SAPO-11(P) Catalyst

P atm	Conv %	Y _{iso} %	S _{iso} %	Monomers %	Distribution of monomers		
					3	2, 4	5, 6, 7
10	84.8	77.4	91.3	61	0.21	0.28	0.51
20	68.7	61.8	90.0	76	0.21	0.27	0.52
30	59.6	55.8	93.5	78	0.22	0.30	0.49

Reaction conditions: temperature 320 °C; Whsv2.0 h⁻¹; H₂/CH 8.7

As shown in **Table2**, the conversion of *n*-C₁₄ and the yield of liquid as well as the yield of isomers increased with decreasing whsv. The retention time of feed on the catalyst increases with the decreasing of whsv, and thus the increase of conversion is expectable.

The influence of H₂/CH ratio on *n*-C₁₄ hydroconversion is shown in **Table3**, the conversion of *n*-C₁₄ decreases with increasing the partial pressure of hydrogen (the H₂/*n*-C₁₄(mole) from 4.3 to 8.7), while the isomerization selectivity increases. The changes are relatively small with a higher WHSV of 4.1h⁻¹. It should be point out that at pretty low H₂/CH ratio, catalyst deactivation became predominant. All these reflect the importance of H₂ in the

* Corresponding author, E-mail: gaozx@sxicc.ac.cn

isomerization process. And the role of H₂ during isomerization might be the same as we have discussed in a previous paper^{1,3}.

Table 2 Effect of WHSV on N-C₁₄ Hydroconversion over 0.4Pt/SAPO-11(P) Catalyst

WHSV h ⁻¹	Y _l %	Conv %	Y _{iso} %	S _{iso} %	Monomers /%	Dis. of monomers		
						3	2, 4	5, 6, 7
4.1	98.4	34.3	32.7	95.3	87	0.20	0.32	0.48
3.0	99.1	44.6	42.6	95.5	85	0.19	0.29	0.52
2.0	98.8	59.6	55.8	93.5	78	0.22	0.30	0.49
1.0	97.6	83.8	74.8	89.2	64	0.22	0.30	0.48

Temperature 320°C Pressure 30atm; H₂/CH 8.7mol/mol

Table 3. Effect of H₂/CH Ratio on the Hydroisomerization of N-C₁₄ over 0.4Pt/SAPO-11(P) Catalyst at 30atm

Temp °C	H ₂ /CH mol/mol	Wshv h ⁻¹	Conv %	Y _{iso} %	S _{iso} %	Monomers %	Dis. of monomers		
							3	2, 4	5, 6, 7
300	4.3	2.0	39.8	33.6	84.6	85	0.21	0.31	0.48
300	8.7	2.0	28.4	25.9	91.5	86	0.23	0.29	0.48
320	4.3	4.1	37.0	33.3	90.2	84	0.21	0.30	0.49
320	8.7	4.1	34.3	32.7	95.3	87	0.20	0.31	0.49

It was found that the catalytic behavior of 0.4Pt/SAPO-11(P) catalyst with time on stream was largely influenced by operating parameters. A larger H₂ partial pressure inhibited the n-tetradecane conversion, while a slower deactivation was observed. Noticeable catalyst deactivation was observed at a lower reaction pressure, especially at atmospheric pressure, while at pressures higher than 10atm, the isomerization process was stabilized in 30 minutes (Fig 2).

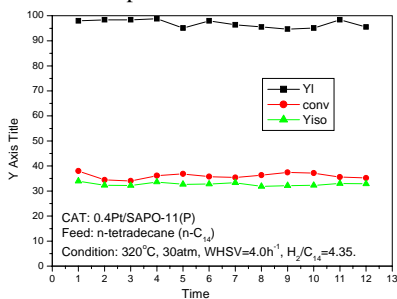


Figure 2 Catalytic performance of 0.4Pt/SAPO-11(P) catalyst in n-C₁₄ hydroconversion. (Yl=Yield of Liquid)

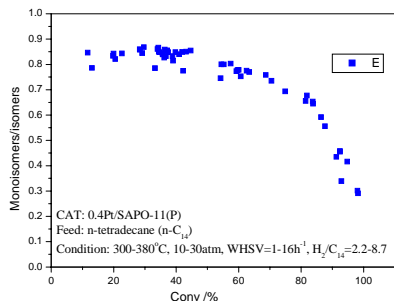


Figure 3. Change of Monoisomers/isomers ratio as a function of the n-tetradecane conversion over 0.4Pt/SAPO-11(P) catalyst

Though the change of reaction variables, such as pressure, whsv and H₂/CH ratio, did affect the distribution of the isomerization products (Table 1-3). It has been found that the distribution can only be correlated with conversion level of n-C₁₄ as shown in Fig.3. The content of mono-isomers in the isomerization products decreases with increasing conversion level, indicating secondary transformation of mono-branched isomers to multi-branched isomers. However, the distribution of mono-branched isomers was found to be independent

of conversion level. In the conversion range up to 90%, the distribution of positional mono-branched isomers changes little (Fig 4). Of the mono-branched isomers, most are central positional methyl branched isomers, namely, 4-, 5-, 6-, 7-methyltridecane, which is highly desired components for diesel and lube base oil.

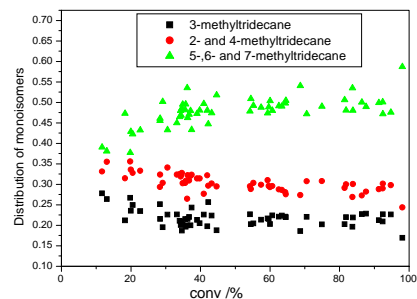


Figure 4. The distribution of mono-branched isomers as a function of n-tetradecane conversion over 0.4Pt/SAPO-11(P) catalyst

Conclusions

An increase of activity was observed with the P modified catalyst, and isomerization selectivity was also improved especially at low temperature with a conversion up to 85%. The content of mono-isomers decreased with increasing conversion levels of n-tetradecane, while the distribution of the mono-isomers changed little. The high Pt dispersion and relatively large amount of weak acidity of P modified Pt/SAPO-11 catalyst account for the improved hydroisomerization performance. Comparing these results with our previous findings, we come to the conclusion that the catalytic behavior is largely influenced by the nature of SAPO-11 molecular sieve.

Acknowledgement. Financial aid from Fushun Petrochemical Company is gratefully acknowledged. The authors thank the State key laboratory of Coal Conversion for basic sample characterizations and collecting the GC-MS data. The authors are indebted to Dr. Zhao Liangfu, Ms. Li Yuan, Ms. Wang Hairong and Mr. Dong Lingyao who participated in this work.

References

- Weitkamp, J., *Ind. Eng. Chem. Prod. Res. Dev.* 1982; 21, 550.
- Zhang W. and Smirniotis P.G. *J. Catal.*, 1999, 182, 400-416.
- Thomson, R.T., Noh, M.M., Wolf, E.E. *Am. Chem. Soc. Symp. Ser.* 1990, 437, 75.
- Choung, S.J., Butt, J.B. *Appl. Catal.* 1990, 64, 173.
- Halik, C., Chaudri, S.N., Lercher, J.A., *J. Chem. Soc. Faraday Trans.* 1989, I 85, 3879.
- Martens, J.A., Grobet, P.J., Jacobs, P.A. *J. Catal.* 1990, 126, 299.
- Thomson, R.T., Wolf, E.E., Montes, C., Davis, M.E. *J. Catal.* 1990, 124, 401.
- Hasha, D., Saddalriaga, L., Hataway, P.E., Cox, D.F. and Davis, M.E., *J. Am. Chem. Soc.* 1988, 110, 2127.
- Geng C.-H., *Ph. D. Thesis*, Institute of Coal Chemistry, Chinese Academy of Sciences, 2003.11.
- Geng, C.-H., Zhang F. Gao, Z.-X., Zhao, L.-F., and Zhou. J.-L., *Proc.3rd Asia-Pacific Congress on Catalysis*, Dalian, China Oct.12-15, 2003; pp804-805.
- Hollo, A., Hancsok, J., Kalló, D. *Appl. Catal. A: General*, 2002, 229, 93-102.
- Chao, K.-J., Lin, C.-C., Lin, C.-H., Wu, H.-C., Tseng C.-W., Chen; S.-H., *Appl. Catal. A: General*, 2000, 203, 211-220.
- Gao, Z.-X., Geng, C.-H., Zhao, L.-F., Zhang F. and Zhou. J.-L., *Proc.4th Korea-China Joint Workshop on Clean Energy Technology*, Jeju Island, Korea. Oct. 2002; pp267-273.

ESTIMATING REACTIVITY OF ASPHALTENES BY A COMBINATION OF QUANTUM CHEMICAL CALCULATION AND STATISTIC ANALYSIS

Xiaoliang Ma*, and Chunshan Song

The Energy Institute, The Pennsylvania State University
409 Academic Activities Building, University Park, PA 16802

*E-mail: mxx2@psu.edu

1. Introduction

Asphaltenes are the most polar and heavy substances existing in petroleum, which cause serious problems in oil recovery, pipelines, and especially in thermal and catalytic processing of petroleum residues due to coking. Many approaches have been examined in molecular presentation of asphaltenes for several decades. Recently, some average molecular structures of asphaltenes have been constructed on the basis of elemental composition, detailed structural parameters from NMR data, pyrolysis gas chromatography/mass spectrometry and others [1-6], which allows one to estimate quantitatively the reactivity of asphaltenes at molecular level on the basis of chemical structural models of asphaltenes.

Some approaches to estimating reactivity of aromatic compounds on the basis of computational chemistry have been reported [7-11]. These approaches incorporated some quantum chemical parameters including ionization potential, bond order, π -electron density or frontier orbitals to estimate the hydrogenation reactivity and electrophilic reactivity, which allows one to compare the reactivity of a family of compounds. However, for estimating the reactivity of asphaltenes, these methods are not directly applicable because 1) asphaltenes are composed of mixtures of hundreds of organic molecules rather than a single macromolecule, 2) there are many reactive sites even in a single macromolecule in asphaltene, and 3) not only HOMO and LUMO but also HOMO-1, HOMO-2, ... and LUMO +1, LUMO +2, ... contribute to the reactivity of the macromolecule since the energy levels of these orbitals are close to the frontier orbitals in the macromolecule of polycyclic aromatics. Consequently, it is necessary to develop a quantitative method to estimate the reactivity of asphaltene on the basis of its chemical structural model. In the present study, we have developed an approach as a new estimation method by using a distribution function of superdelocalizability to estimate the reactivity of asphaltenes. This method combines the quantum chemical calculations and statistic analysis.

2. Structural Models of Asphaltenes

The chemical structural models for three asphaltenes, Khafji ($C_{142}H_{157}N_2O_2S_4$), Maya ($C_{125}H_{134}N_2O_3S_3$) and Iranian ($C_{109}H_{108}N_2O_3S_3$), are shown in Figure 1. The model for each asphaltene contains three macromolecules, representing an average chemical structure of the asphaltene. These models were constructed by researchers at National Institute of Advanced Industrial Science and Central Research Laboratories, Idemitsu Kosan Company, on the basis of the analytical data (including ultimate analysis, 1H -NMR, ^{13}C -NMR and laser desorption mass spectrometry) of the asphaltenes obtained respectively from fractionation of Khafji, Maya, and Iranian vacuum residues using n-heptane as a solvent [2,12].

3. Computational Methods

All quantum chemistry calculations in this study were performed by using a semi-empirical molecular orbital method, the

PM3 parameters, in CAChe version 5.0. Geometries of the asphaltene macromolecules and some aromatics were optimized. Bond order, net atomic charges, ionization potential, electrophilic frontier density and electrophilic superdelocalizability were calculated. The electrophilic superdelocalizability was defined as:

$$S^E(x) = 2 \sum_{i=1}^N [\phi_i(x)^2] / (\alpha - E_i)$$

Here, N is the total number of the occupied orbitals, $\phi_i(x)$ is the value of the filled orbital i at point x , E_i is the energy of that orbital in electron volts (eV), α is the reagent energy [13, 14]. The statistic analysis was performed by using a frequency function in Microsoft Excel.

4. Results and Discussion

Correlation of Hydrogenation Reactivity of Aromatics with the Calculated Parameters There are not many comparable quantitative data in the literature for hydrogenation reactivity of aromatic hydrocarbons. A set of pseudo-first-order rate constants for hydrogenation of benzene, biphenyl, naphthalene and 2-phenylnaphthalene catalyzed by Co-Mo/Al₂O₃ were determined by Spare and Gates [15]. In order to determine which calculated parameter is more sensitive to hydrogenation reactivity, bond order, ionization potential, electrophilic frontier density and electrophilic superdelocalizability (ESD) for the four aromatic hydrocarbons were calculated and correlated with their hydrogenation rate constants. The results revealed that ESD values of the aromatic hydrocarbons show a better correlation with their hydrogenation reactivities, indicating that we can use ESD values as an index for hydrogenation reactivity. This is probably because the π -complex intermediates formed in hydro-generation process transfer electrons from the higher occupied molecular orbitals of the hydrocarbons to an unoccupied d-orbital on the metal. The higher ESD values result in a more facile electron transfer from the hydrocarbons to the metal, and thus, a stronger adsorption of the hydrocarbons on the active sites on the catalyst surface.

Estimating Hydrogenation Reactivity of Asphaltenes by a ESD Distribution Function The ESD values for all atoms in three asphaltene models were calculated. As well known, it is unsuitable to compare the hydrogenation reactivity of asphaltenes by only comparing the reactivity of one or a couple of sites in each asphaltene model or by only comparing the reactivity of a macromolecule in each asphaltene. In order to solve this problem, we built a distribution function of ESD values for the three asphaltenes on the basis of the structural models. The higher percentage of the atoms in a range of high ESD value indicates the higher hydrogenation reactivity of the asphaltene. Percentage of the atoms in each asphaltene structural model as a function of ESD value is shown in Figure 2. The percentage of the atoms with ESD value higher than 1 increases in the order of Maya < Khafji < Iranian, indicating that the hydrogenation reactivity of the asphaltenes increases in the same order. A distribution function of the bond order for three asphaltenes were also calculated and the results imply a similar trend for hydrogenation reactivity. The distribution function of the bond order also shows that there are higher percentages of weaker C-C bonds in Khafji asphaltenes than in the others, indicating its higher thermal

cracking reactivity. The estimated hydrogenation reactivity and thermal cracking reactivity in the present study are in agreement with the experimental results obtained by Central Research Laboratories, Idemitsu Kosan Company [16]. It has been shown in previous studies that asphaltenes from different Company sources show different reactivities in catalytic and thermal hydroprocessing [17,18].

5. Acknowledgment

We gratefully acknowledge the financial support by Idemitsu Kosan Company and New Energy and Industrial Technology Development Organization (NEDO). We thank Mr. R. Tanaka, Dr. T. Takanohashi and Dr. S. Sato for providing the structural models of the three asphaltenes and for helpful discussions.

6. Reference

- Shen, Y.; Mullins, O. C. Eds. *Asphaltenes, Fundamentals and Applications*, Plenum Press, New York, London, 1995.
- Sato, S., *Sekiyu Gakkaishi*, 1997, 40, 46.
- Artok, L.; Su, Y. Hirose, Y.; Hosokawa, M.; Murata, S.; Nomura, M. *Energy & Fuels* 1999, 13 287.
- Groenzin, H.; Mullins, O. C. *Pet. Sci. Technol.* 2001, 19, 219.
- Sheremata, J. M.; McCaffrey, W. C.; Gray, M. R. *Prepr., Div. Fuel Chem., Am. Chem. Soc.* 2001, 46, 351.
- Sato, S.; Takanohashi, T. Tanaka, R. *Prepr., Div. Fuel Chem., Am. Chem. Soc.* 2001, 46, 353.
- Geneste, P.; Amblard, P.; Bonnet, M.; Graffin, P. J. *Catal.* 1980, 61, 115.
- Nag, N. K. *Appl. Catal.* 1984, 10, 53.
- Ma, X.; Sakanishi, K.; Isoda, T.; Mochida, I. *Energy & Fuels* 1995, 9, 33-37.
- García-Cruz, I.; Martínez-Magadá, J. M. Guadarrama, P.; Salcedo, R.; Illas, F. J. *Phys. Chem. A* 2003, 107, 1597-1603.
- Marston, G.; Monks, P.; Wayne, R. P. Correlations between Rate Parameters and Molecular Properties, in *General Aspects of the Chemistry of Radicals*, Alfassi, Z. B. Ed.; John Wiley and Sons: New York, 1999, p.429.
- Takanohashi, T. Sato, S.; Tanaka, R., *Fuel Chem. Div. Preprints* 2001, 46(2), 357.
- Fukui, K.; Yonezawa, T.; Nagata, C. *Bull. Chem. Soc. Japan*, 1954, 27, 423.
- Fukui, K.; Yonezawa, T.; Nagata, C. *J. Chem. Phys.*, 1957, 26, 831.
- Sapre, A. V. Gates, B. C. *Ind. Eng. Chem. Process Des. Dev.* 1981, 20, 68-73.
- Tanaka, R., personal communication, 2003.
- Song, C.; Nihonmatsu, T.; Nomura, M. *Ind. Eng. Chem. Res.*, 1991, 30 (8), 1726-1734.
- Song, C.; Hanaoka, K.; Nomura, M. *Energy & Fuels*, 1992, 6 (5), 619-628

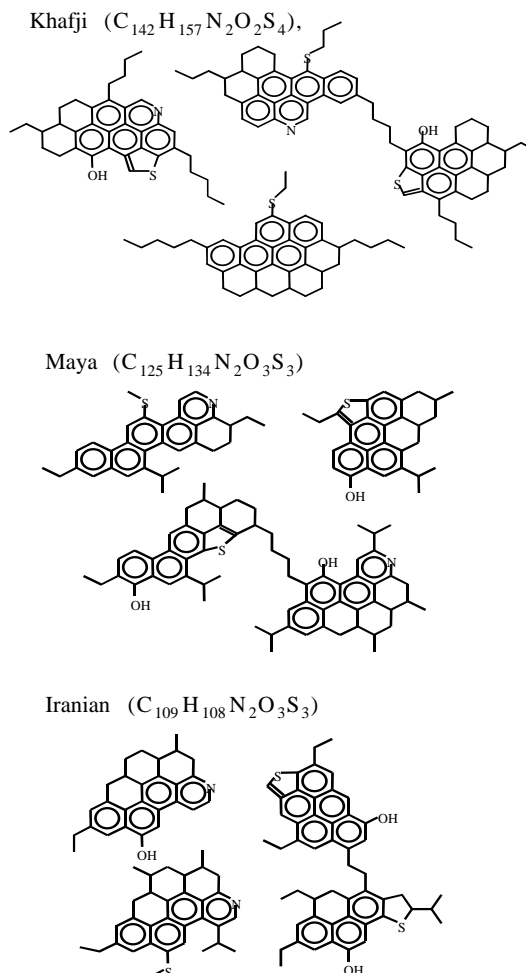


Figure 1. Chemical structural models of three asphaltenes

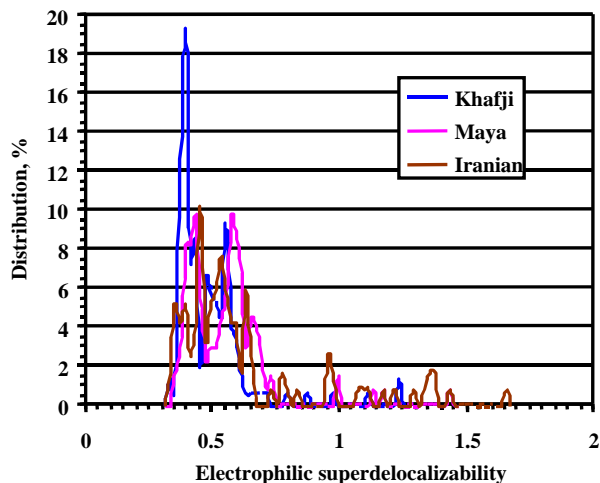


Figure 2. Distribution of electrophilic superdelocalization values on three asphaltenes

Hydrogenation of naphthalene on HY/MCM-41 supported sulfided-NiMo catalysts

LIU Yunqi LI Wangliang, LIU Chunying Cui Min, LIU Chenguang

College of Chemistry & Chemical Engineering,
University of Petroleum, China, Dongying,
Shandong257061

E-mail liuyq@mail.hdpu.edu.cn

Abstract:

A series of mesoporous molecular sieves MCM-41 with different Si/Al molar ratios were synthesized by hydro-thermal method. The influence of aluminum contents on the properties and pore structure of MCM-41 molecular sieves were investigated. The supported Ni-Mo catalysts with MCM-41 and γ -Al₂O₃ as supports were synthesized by impregnating with Ni-Mo-P solution. The activity of the catalysts was characterized by hydrogenation of naphthalene. The influence of Si/Al ratio of MCM-41 on hydrogenation activity of the catalysts was investigated. The results indicated that the relative crystallinity of MCM-41 decreases with the increase of aluminum content in the molecular sieves; however, the hydrogenation activity of the catalysts, especially the ring-opening activity, increases with the increase of aluminum content. The synergistic effect for hydrogenation of naphthalene was found by mixing MCM-41 and HY molecular sieves. At 360°C, the catalysts with HY and MCM-41 mixture as supports has higher activity. The reaction network for hydrogenation of naphthalene includes two parallel pathways; naphthalene was hydrogenated to tetralin, then the isomerization and ring-opening of tetralin occurred, or tetralin was further hydrogenated to decalin, followed by the isomerization and ring-opening of decalin.

Key words: MCM-41 molecular sieve, naphthalene, hydrogenation, activity, reaction mechanism

1. Introduction:

There is an increasing demand for environmentally friendly hydrocarbons and clean-burning high performance fuels, such as distillate fuels like diesel and jet fuels. Distillate fuels typically contain paraffins, naphthenes, and aromatics. For fuels quality parameters such as cetane, gravity and emissions, paraffins are the most desirable components, followed by naphthenes, followed by aromatics. The least desirable are multi-ring aromatic compounds. Owing to more and more strict environmental and clean-fuel legislation, deep hydrodearomatization of diesel has been the focus of many recent studies. Many approaches has been applied in the synthesis of catalysts such as using different types of zeolite as supports^[1], adding promoters^[2], etc.

MCM-41 mesoporous molecular sieve has become one of the world-wide known materials since 1992 for its high surface area and meso-size porosity^[3]. MCM-41 has shown its advantages in the fields of catalysis, material and organic compounds synthesis^[4,5]. Corma et al^[6] reported that the activity on one stage mild hydrotreatment of vacuum gasoil on NiMo catalysts supported on MCM-41 molecular sieves, is superior in HDS, HDN and HC reaction, compared to that of catalysts with the same Ni, Mo

content supported on amorphous-alumina or on USY zeolite. T. Halachev^[7] reported the catalytic activity of (P)NiMo/Ti-HMS and (P)NiW/Ti-HMS catalysts in the hydrogenation of naphthalene. Condam et al^[8] found that cis- and trans-declins easily produced on Pt/MCM-41 compared to Pt/Al₂O₃ and Pt/TiO₂. In this paper, we have synthesized a series of Al-MCM-41 with different Si/Al ratios and investigated the performance of hydrogenation of naphthalene on MCM-41 supported sulfided-NiMo catalysts. Based on the relative weak acidity on Al-MCM-41, we also investigated the catalytic performance of modified sulfided-NiMo catalysts supported in mixed Al-MCM-41 with the HY zeolite. For the modified catalysts, the activity and ring-opening products concentration increase with the addition of HY zeolite. These results are beneficial from the synergistic effect of combination microporous with mesoporous zeolites.

2. Experimental

2.1 The preparation of MCM-41 with different Si/Al ratios

Al-MCM-41 with Si/Al ratios of ∞ , 60, 50, 40, 25 were synthesized following the procedure given in Ref[1] using hexadecyltrimethylammonium bromide (purity $\geq 99\%$) as template, sodium silicate solution (SiO₂ $\geq 24.19\%$) as silica source and pseudoboehmite as aluminum source. The sol-gel was crystallized under 120°C in 24h. The as-synthesized material was calcinated in a N₂ atmosphere at 550°C during 1h followed by a 6h calcinations in the air at the same temperature.

2.2 The preparation and characterization of catalysts

The supports were prepared in the following procedure: molding, desiccation, ion-exchanging with 1 mol.l⁻¹ NH₄NO₃ solution for 3 times and calcinations. The catalysts Al-MCM-41 and catalysts modified by adding HY zeolite (15%) were compared to the reference catalysts (Mo-Ni-P/HY(15%)-Al₂O₃). Mo-Ni-P catalysts were prepared by the incipient wetness impregnation technique with the required amount of an aqueous solution of ammonium heptamolybdate, base nickel carbonate and phosphoric acid to obtain catalysts. By these strategies, we prepared three different kinds of catalysts: (1) sulfided-NiMo supported on different MCM-41 (Si/Al = ∞) content (0, 20%, 40%, 60%); (2) Al-MCM-41 supported sulfided-NiMo catalysts with different metal oxides content (20%, 26%, 32%, 40%); (3) sulfided-NiMo supported on mixed support of combination Al-MCM-41 with HY zeolite

X-ray powder diffraction (XRD) were carried on D/Max-III type spectrometer with Cu K α radiation, Voltage is 40KV and electrical current 40mA. Surface area, pore volume and average pore diameter were calculated from the adsorption-desorption isotherms of N₂ at 77.35K on a ASPA-2010 adsorption apparatus. The acidity of molecular sieves and catalysts were measured by adsorption-desorption of pyridine. The alumina content in the MCM-41 molecular sieves was measured by chemical-titration method^[9].

Reaction system and procedure

2.3 The evaluation of catalytic performance and products identification

The experiments of evaluation of catalytic performance were performed in a fixed bed stainless tubular reactor (10mm internal

diameter and 0.8ml length) in a micro-reactor. The catalysts were pre-sulfided before hydrodearomatization reaction by using CS₂ at 4 MPa under 340 °C for 3h. The reaction condition for hydrodearomatic were 340-370 °C, H₂ pressure is 4.0MPa, H₂/Oil ratio is 500, WHSV=1h⁻¹. The products were analyzed by a Varian-3400 gas chromatography equipped with a 0.25mm×30m HP CP-1 capillary column and a flame ionization detector and the product identification was carried out by gas chromatography-mass spectrum (GC-MS).

3. Result and discussion:

3.1 The effect of sol-gel Si/Al molar ratio on MCM-41 structure

Fig.1 shows the XRD pattern of pure silica MCM-41 and Table1 depicts the influence of the feed Si/Al ratio on the XRD peak intensity of 100 plane and other properties of MCM-41. A decrease in Si/Al ratio decrease the intensity of the main XRD peak, indicating that increasing Al content of the feed hindered the crystallization process. In Fig.2, the pore diameter distribution of a typical as-synthesized MCM-41 has figured out and the open pore size focus on 2.8-3.0nm.

From table 1 it can be seen with the aluminum added in MCM-41, relative crystalline of molecular sieves decrease, that is because aluminum inserting into Si-O tetrahedron can cause lattice disfigurement and have bad effect to hexagon structure. With the increase of aluminum in MCM-41 the acidity of molecular sieves increase.

3.2 The product identification of hydrodearomatization of naphthalene

The product identification was made by GC and GC-MS analysis. Figure3 shows a typical GC chromatogram of the product. Some products were identified by comparison of GC retention time with those of the standard samples, Other products were identified by GC-MS, which data system searches automatically the associated database spectra of molecules and gives a best fit match.

3.3 The effect of total H₂ pressure on naphthalene conversion and products distribution

To investigate the effect of total H₂ pressure on naphthalene conversion and products distribution. We selected a Catalyst with the formula of MoNi(P)/MCM-41 (20%, Si/Al=∞)-Al₂O₃ and test temperature condition is 370 °C, the ratio of H₂ and oil is 500, WHSV is 1.0h⁻¹. From Fig.3 it can be seen that the naphthalene conversion increase with the increase of total H₂ pressure. This is because naphthalene hydrogenation and deep-hydrogenation reaction consume hydrogen which causes the molar of gas decrease. From the equilibrium of the reactions the conclusion can be drawn that increasing H₂ pressure is benefit for naphthalene conversion. Fig 4 shows that the effect of H₂ pressure on the products distribution of naphthalene hydrogenation products

The products can be divided into three parts, which are the tetralin and its isomers, decline and its isomers and ring-opening products. The former two parts is from the hydrogenation pathway and ring-opening products is from the hydrocracking pathway. From Fig.4 it can be seen that naphthalene conversion and the activity of deep-hydrogenation and ring-opening increase

with the increase of total H₂ pressure. Increasing total H₂ pressure is good for naphthalene conversion, ring-opening reaction and cetane number improvement.

3.3 The effect of metal content on the naphthalene conversion and products distribution

The MCM-41 is a kind of mesoporous zeolite with high surface area and large pore diameter. This is easy for high concentration active components to disperse on its surface. From Table3 it can be seen that the catalysts activity increase with the increase of metal content. As a result naphthalene conversion increases and deep-hydrogenation products such as decalins and ring-opening increase. But the metal content in the catalysts increases to 40%, the activity of catalyst decrease. The possible reason is that excessive metal may form big particles which deposit on the catalysts. This can block the aperture of catalysts and confine the diffusion of reactant.

3.4 The acidic component of supports on the naphthalene conversion and products distribution

From the above results it can be seen that the acidity on the MCM-41 is too weak which causes the number of acidity sites are too small and the acidity strength of catalysts are too weak. This does no good to naphthalene deep-hydrogenation and ring-opening. As a result the main products on NiMo/MCM-Al₂O₃ are tetralins while declins and ring-openings are not as many, which just cause a little increase of cetane number. In order to improve the performance in catalytic ring-opening reaction, it is necessary to add the acidic component. HY is a microporous zeolite and its acidity is stronger than MCM-41. So we selected HY molecular sieve as acidic component and added it in the supports. From the Table it can be seen that naphthalene conversion increased with the HY content added to the catalysts increase. The catalysts1 with HY/MCM-41/Al₂O₃ in the support have the high conversion. Catalysts 2 with only HY/MCM-41 have the highest ring-opening content This can be attributed to the interaction of HY acidic component and the synergistic effect for hydrogenation of naphthalene was found by mixing MCM-41 and HY molecular sieves.

Conclusions

1. A series of MCM-41 molecular sieves with different Si/Al molar ratio were synthesized by hydrothermal method. With the decrease of Si/Al, alumina oxide content and acid sites increased while the relative crystallinity decreased.
2. Total H₂ pressure plays an important role in naphthalene hydrogenation. With pressure increased the activity of deep-hydrogenation and ring-opening increase sharply.
3. The conversion of naphthalene increase with metal oxides active components content on the catalysts with the supports MCM-41 mesoporous zeolites increased
4. Catalysts added HY zeolites naphthalene deep-hydrogenation, especially the ring-opening properties increase.

References

- [1] Corma A., Martinez A, et al, Catalytic performance of new dealuminated ITQ-2 zeolite for mild hydrocracking and aromatic hydrogenation processes, *Journal of Catalysis*, 2001, 200, 295~269
- [2] Brunn, et al, January 24, 1984, United States Patent, 4427534
- [3] Beck J S, Vartuali J C, et al., A new family of mesoporous molecular sieves prepared with liquid-crystal template, *J. Am. Chem. Soc.*, 1992, 114:10834~10843
- [4] Schmidt R, Stocker M, et al, MCM-41: a model system for adsorption studies on mesoporous materials, *Microporous Mater.*, 1995, 3:443~448
- [5] Xu X Z, Su J M, Da J W, Test on FCC catalyst containing MCM-41 zeolite in a semi-commercial unit, *Petroleum Processing and Petrochemical (Chinese)*, 2001, 32 (8) : 46~50
- [6] A. Corma, A. Martinez, et al., Hydrocracking of vacuum gasoil on the novel mesoporous MCM-41 aluminosilicate catalyst, *Journal of Catalysis*, 1995, 153, 25~31.
- [7] Halachev T, Nava R, Dimitrov L, Catalytic activity of (P)NiMo/Ti-HMS and (P)NiW/Ti-HMS catalysts in the hydrogenation of naphthalene, *Applied catalysis A: General* 1998, 169, 111~117
- [8] Reddy C M, Song C S, Synthesis of mesoporous molecular sieves and their application for catalytic conversion of polycyclic aromatic hydrocarbons, *Preprints, Am. Chem. Soc. Div.*, 1996, 41(3):906~909
- [9] Feng Chengwu et al, *Analytical Chemistry Experiment*, Publishing House of University of Petroleum (East China), 1995, 229~231

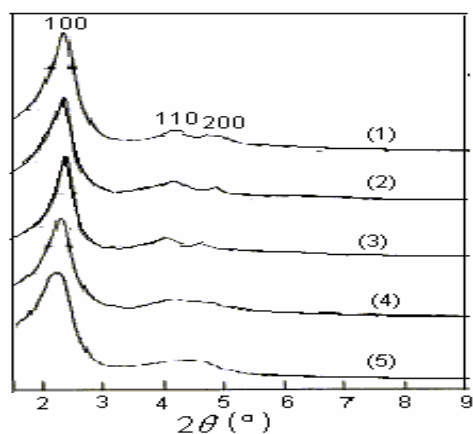


Fig.1 XRD pattern of as-synthesized MCM-41 molecular sieves
 (1) Si/Al=∞; (2) Si=60; (3) Si=50; (4) Si=40; (5) Si=25

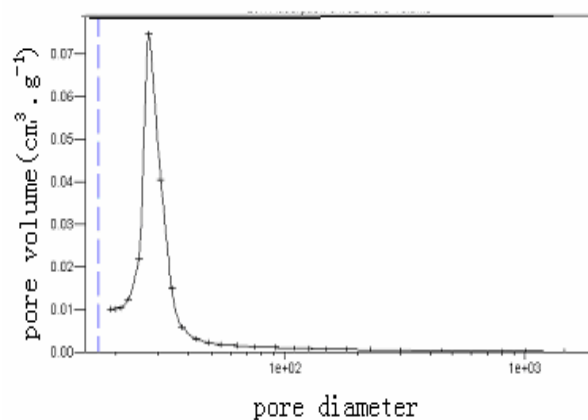


Fig.2 Pore diameter distribution of typical as-synthesized MCM-41

Table 1 Effect of Si/Al molar ratio on structure of MCM-41

Si/Al, molar ratio	∞	25	40	50	60
$2\theta, ^\circ$	2.104	2.078	2.231	2.191	2.143
XRD					
Relative crystallinity*, %	100	89.8	85.4	82.4	80.7
d_{100}, nm	4.193	4.245	3.956	4.028	4.114
Half brand width, nm	0.320	0.320	0.320	0.340	0.340
Surface area, $\text{m}^2 \cdot \text{g}^{-1}$	791	1294	860	794	770
BET					
Pore volumn, $\text{cm}^3 \cdot \text{g}^{-1}$	0.57	1.05	0.68	0.64	0.66
Pore diameter, nm	2.8	3.2	3.1	2.7	2.9
Acidity, m%	18.4	29.5	26.3	24.7	21.3
W(Al_2O_3), m%	—	3.76	1.62	1.50	1.37

Relative crystallinity: the crystallinity of MCM-41(Si/Al=∞) is 100 while others are relative to this value

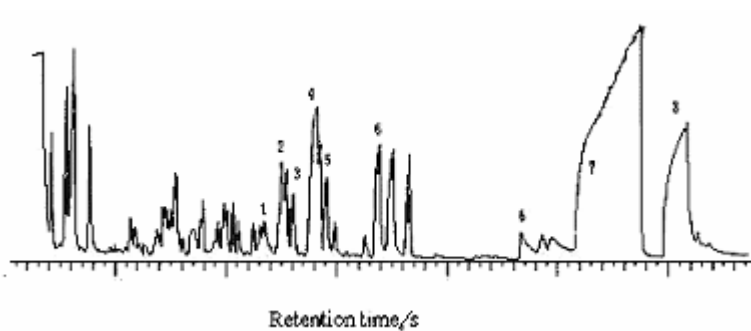


Fig. 3 GS-MS of the products for hydrogenation of naphthalene 1-butylcyclohexane; 2-cis-decaline; 3-methylindane and its isomers; 4-trans-decaline; 5-butylbenzene; 6-methylindene and its isomers; 7-tetralin; 8-naphthalene

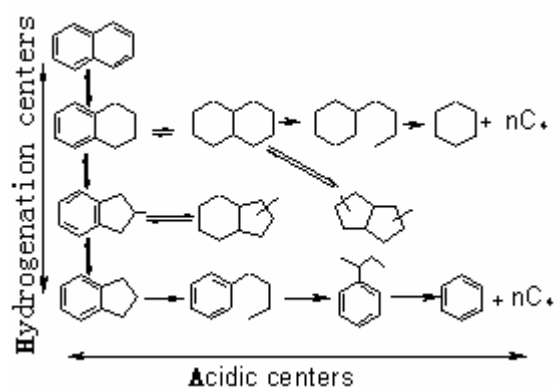


Fig.4 Reaction pathways for hydrogenation of naphthalene sulfurized CoMo catalysts

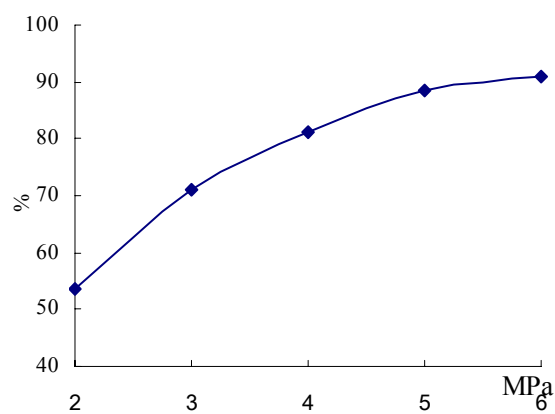


Fig.3 The effect of pressure on the conversion of naphthalene

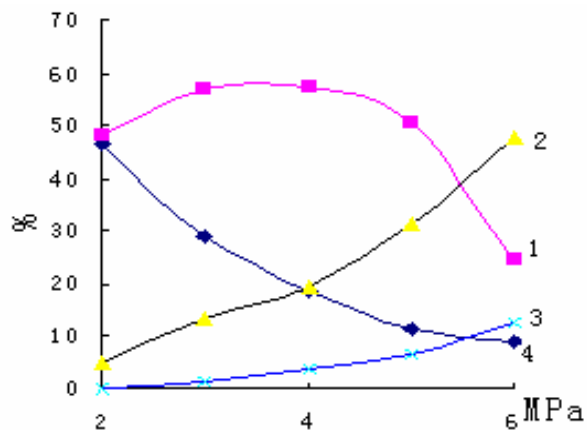


Fig.4 The effect of H₂ pressure on the distribution of products
 1—tetralin and its isomers; 2—declins and its isomers; 3—ring-opening products; 4—naphthalene

Table 3 : the effect of metal content on the naphthalene hydrogenation

Metal content, (NiO+MoO ₃), m%	W(production), m%				Conversion, %
	Naphthalene	Tetralins	Decalins	Openings	
20	16.96	66.97	9.69	5.34	83.04
26	14.63	63.69	12.23	9.45	85.37
32	9.69	62.06	17.89	9.79	90.31
40	11.84	55.14	23.68	8.45	88.16

Table 4 The properties of catalysts added HY zeolite

Catalysts	T, °C	W(products), %				Conversion, %
		Naphthalene	Tetralins	Declins	Other products	
Reference	340	13.88	24.29	27.00	32.66	86.12
	350	16.81	27.14	30.73	23.37	83.19
	360	18.62	20.13	34.78	22.18	81.38
Catalyst 1	340	6.91	60.23	16.05	17.35	93.09
	350	7.23	49.87	21.21	19.27	92.77
	360	10.24	40.24	19.58	25.32	89.76
Catalysts 2	340	9.45	39.52	18.83	29.60	91.55
	350	11.25	32.10	18.23	35.46	88.75
	360	13.77	24.71	13.97	40.72	86.23

Reference catalyst: Mo-Ni-P/HY(15wt%)-Al₂O₃

Catalyst 1: Mo-Ni-P/MCM-41(45wt%)-HY(15wt%)-Al₂O₃

Catalyst 2: Mo-Ni-P/ HY(20 wt%)- MCM-41

DOWNHOLE UPGRADING OF WOLF LAKE OIL USING THAI/CAPRI PROCESSES - TRACER TESTS

Malcolm Greaves and TianXiang Xia

Improved Oil Recovery Group, Department of Chemical Engineering,
University of Bath, Bath BA2 7AY, England
Tel: 44 1225 826624 Email: M.Greaves@bath.ac.uk

Keywords: In situ combustion, air injection, heavy oil, in situ upgrading, THAI, CAPRI

Introduction

With worldwide conventional oil production expected to peak during the present decade, the need to reevaluate heavy oil resources is becoming more imperative. The vast heavy oil and tar sands resources in Canada, Venezuela, the United States and other parts of the world will play an important role in sustaining our future energy supply¹.

THAI – ‘Toe-to-Heel Air Injection’ is an integrated reservoir-horizontal wells process, which uses air injection to propagate a combustion front from the toe-position to the heel of the horizontal producer (HP). Fig 1 is a schematic representation of the basic features of the process².

THAI is a stable and robust in-situ combustion process, as defined by the absence of oxygen breakthrough at the production well, as well as no tendency for severe gas overriding³. The stability of the THAI process depends on two key factors: (1) a high temperature burning zone, which is more advanced in the top part of the oil layer, exhibiting controlled (stable) gas override behaviour, and (2) deposition of coke, or heavy residue, inside the HP. The coke which is deposited inside the HP acts as a gas seal.

THAI is a new, more advanced variant of the conventional in-situ combustion (ISC) process, which operates as a short-distance, as opposed to long-distance displacement process⁴. Due to the well arrangement used in THAI, the mobilised oil ahead of the combustion front only travels a short distance (down) to the exposed section of the HP. Since THAI operates at much higher temperatures than SAGD, it can achieve significant in-situ upgrading, and thereby maximize oil recovery. THAI is currently the subject of a pilot development at Christina Lake, Canada (2005).

CAPRI is the catalytic extension of the THAI process, incorporating an annular layer of catalyst, emplaced on the outside of the perforated horizontal producer well, along its whole length^{5, 6}. The reaction conditions created ahead of the combustion front, prior to reactants passing down through the mobile oil zone to contact the catalyst, are established by the THAI process. Further upgrading of the produced oil is achieved by catalytic conversion, as the mobilised oil passes through the catalyst layer.

Although, extensive tests on the performance of THAI and CAPRI have been made, only basic upgrading data have been reported so far. The present study aims to quantify the extent and nature of the oil upgrading during an experiment dry and wet phases of THAI and CAPRI. Gas, oil, water and solid residue analyses are used to infer mechanisms of upgrading and to begin to gauge the economic (sweep and recovery) and environmental (gas emissions and produced water quality) impact associated with the eventual field operation of the process.

Experiments

Two three-dimensional in situ combustion tests were carried out in a rectangular, low pressure stainless steel cell, measuring 0.6 m x

0.4 m x 0.1 m, equipped with ports for air injection and production. Heavy Wolf Lake crude oil (10.5 °API) was mixed with wet sand prior to packing into the cell, representing a homogeneous oil reservoir. A NiMo hydrodesulfurization (HDS) catalyst was packed around the downstream half of the horizontal producer, as shown in Fig. 2. The tests were designed in such a way as to incorporate both THAI and CAPRI modes in a single test.

Details of the construction of the 3-D combustion cell and operation have been reported previously^{2, 6}. The test conditions are listed in Table 1. Synthetic brine was used in the first THAI/CAPRI test (Run 2000-07), in order to simulate the connate water in the reservoir formation. In the second test (Run 2001-01), a tracer was added to the oil, consisting of a mixture of hydrocarbons (see Table 2). The purpose of the organic tracer was to investigate the mechanisms for oil upgrading achieved during the THAI and CAPRI processes.

It should be noted that the sandpack used in these tests did not contain kaolinite. While 3% kaolinite was added into the sandpacks used in all previous 3-D cell tests, more closely simulating an oil reservoir. The Canadian heavy oil reservoirs typically contain 5% ~ 10% of clays, such as kaolinite, illinite, montmorillonite, and chlorite⁷. It is well-known that kaolinite is a thermal cracking catalyst. Therefore, the present series of experiments represents the a worst case scenario for thermal upgrading of heavy oil by THAI-CAPRI.

Results and Discussion

The main results from the two THAI/CAPRI tests are summarised in Table 3.

Run 2000-07. This was a combined dry and wet THAI/CAPRI test, in which deuterated water was injected together with the injected air (CAPRI), as tracer during the second wet combustion period. The performance of the combustion process obtained in this test was similar that observed from standard 3-D combustion cell test on Wolf Lake heavy oil (sandpack containing 3% kaolinite)². A stable, high temperature combustion front (500~600°C) was propagated along the HP, during the dry and wet combustion periods. The excellent sweep of the combustion front, in a ‘Toe-to-Heel’ manner, achieved a high oil recovery, at 87% OOIP.

Figure 3 shows the variation of the API gravity and viscosity for samples of the produced oil collected during the experiment. Before the combustion front reached the catalyst layer, the degree of thermal upgrading of the produced oil was only about 2 API points. This is very low, compared to a normal THAI test on Wolf Lake heavy oil. This is because no clay was added into the sandpack for Run 2000-07.

The effect of catalyst on the produced oil is clearly evident in Figure 3. The API gravity of the produced oil jumped from an API value of 14, up to 24, during the period of 240 to 400 minutes. As the combustion front approached the catalyst section along the HP, mobilized oil, already partially upgraded in the THAI process, underwent further catalytic conversion reactions. During the second wet combustion mode, with deuterated water injection, the upgrading trend was reduced slightly from 22 °API to 20 °API. The viscosity of the produced oil achieved by CAPRI was 10 ~ 40 mPas, down from the original 24,400 mPas for Wolf Lake Crude Oil.

Run2001-01. The Wolf Lake oil was ‘spiked’ with the hydrocarbon mixture, before it was mixed with the previously wetted sand for the THAI/CAPRI test. The performance of this test was similar to Run 2000-07. The cumulative oil recovery achieved was also very high, at 82% OOIP, again because of the high effective ‘toe-to-heel’ sweep of the combustion front (500~600°C) through the

sandpack. The produced oil was also upgraded to 23 API point, mainly during the CAPRI test.

In addition to post-mortem insoection of the collected liquid and solid samples, a number of further analyses on the bulk materials were conducted. Metals analysis and molecular analysis were performed on the selected samples of gas, oil, water and solid residues from Run 2001-01 (see Table 4). The results are discussed below.

SARA/PIN. Improvement in the produced oil quality during THAI/CAPRI is quantified using SARA(Saturates, Aromatics, Resins, Asphaltenes) and PIN (Paraffins, iso-Paraffins, Naphthenes). This HPLC procedure shows some variability, but no substantial change through the THAI stage. However, there is a substantial increase in the more desirable oil component (saturates) during the CAPRI stage. It is noticeable that Resins + Asphaltenes fractions decrease substantially (Figure 5), indicating the conversion of these groups to saturates, is one possible mechanism for oil upgrading.

Elemental analysis. This can be used a measure of carbon rejection, or hydrogen addition, associated with oil upgrading (see Table 4). Elemental sulfur decreases once the THAI wet stage commences, but is maintained at lower levels through the CAPRI stage. The maximum sulfur reduction of 39% was achieved in the CAPRI stage. The onset of lower sulfur numbers with start of water injection suggests a mechanism of hydrogen donation from the water, or water-gas-shift reactions in the presence of exposed sulfur (after cleavage of S-C bonds) and evolution as H₂S (hydrodesulfurization). This appears to be effective prior to the combustion front encountering with the HDS catalyst. A similar mechanism might be relevant for nitrogen, which is reduced to nearly one fifth of its original level.

Distribution of organic tracer compounds. The distribution of tracer compounds in the produced oil from Run 2001-01 was measured by GCMS. The ratio of tracer concentration, to that in the original 'spiked' oil, is shown in Figure 6. The increase in n-paraffins just before the start of water injection in THAI is considered a significant indicator of hydrous pyrolysis as an upgrading mechanism. Because normal alkanes have been reduced in-reservoir from the Wolf Lake oil (via biodegradation), these compounds must have been generated de novo. Hydrous pyrolysis of asphaltenes is the proposed mechanism as normal alkenes are virtually absent and the abundance of normal alkanes increases during the wet stages. Changes in the relative abundance of the introduced compounds are variously attributed to continuous (*n*C₁₁, alkylphenyls) or episodic (and *n*C₂₀) distillation, cracking and converting to derivative products (squalane, perhydrofluorene), cracking with polymerization downstream with subsequent cracking later in the run (decylthiophene, dimethyldibenzothiophene).

The coincidence of increased normal alkane generation during the THAI and CAPRI wet phases supports a hydrous pyrolysis (kerogen or oil + H₂O → CO₂ + H₂) or the water-gas shift reaction (CO + H₂O → CO₂ + H₂). Coke gasification coupled with the water-gas-shift reaction could accompany this mechanism or become dominant in the near vicinity of the combustion front, particularly in the CAPRI stage.

Conclusion

In situ upgrading of heavy oil using THAI (thermal) and CAPRI (thermal-catalytic) processes achieves substantial upgrading of produced oil and as well as high oil recovery, up to 87%OOIP. The results of two tracer THAI/CAPRI tests indicate that hydrous pyrolysis of asphaltenes and the water-gas shift reaction are the main

mechanisms, or routes of hydrogenation of the thermally or catalytically cracked oil, producing alkenes in the upgraded oil. The distillation effect of the light fraction also contributes to some (small amount) of upgrading of the produced oil.

The catalytically upgraded oil contains substantially higher levels of saturates and reduced heavy ends. There are also significant environmental benefits because of the large reduction in heavy metals and sulphur, with potential reductions in refinery loadings. Thus, THAI and CAPRI processes are likely to make an important contribution towards sustainable energy supply in the near future.

Acknowledgement. The authors are grateful to the Engineering and Physical Sciences Research Council (EPSRC), United Kingdom, for supporting the THAI and CAPRI research at the University of Bath, via Research Grants: GL/L71773 and GR/M93017. We would like to thank S.W. Imbus and V.P. Nero (ChevronTexaco Energy Research Technology Co., Houston, TX USA) for providing the tracer compounds for the THAI/CAPRI tests and carrying out the analyses, as well as valuable discussion.

References

- (1) Lanier, D.: "Heavy oil – A major energy source for the 21st century", Paper No. 039, *Proc.*, 7th. UNITAR International Conference on Heavy Oil and Tar Sands, Beijing, China, 27-30 October (1998)
- (2) Xia T X, Greaves M., Turta A T, and Ayasse C.: "THAI – A 'Short-Distance Displacement' In Situ Combustion Process for the Recovery and Upgrading of Heavy Oil", *Trans. IChemE*, (2003) *March*, 81(A) pp295-304
- (3) Xia T X, Greaves M and Turta A.: "Main Mechanism for Stability of THAI – 'Toe-to- Heel Air Injection', Paper 2003-30, Canadian International Petroleum Conference, Calgary, Canada, 10-12 June (2003).
- (4) Xia T X and Greaves, M.: "Upgrading Athabasca Tar Sand Using Toe-to-Heel Air Injection", *J. Can. Pet. Tech.*, (2002) **41**, No. 8, 51-57.
- (5) Greaves, M, Abdul El-Saghr and Xia, T. X.: "CAPRI Horizontal Well Reactor for Catalytic Upgrading of Heavy oil", ACS Symposium, Division of Petroleum Chemistry, on Advances in Oil Field Chemistry: Downhole Upgrading, 20-25, Washington, DC, August, (2000). [ACS PREPRINTS, Vol. 45, No. 4, pp595-598]
- (6) Xia T X and Greaves M.: "3D Physical Model Studies of Downhole Catalytic Upgrading of Wolf Lake Heavy Oil Using THAI", *J. Can. Pet. Tech.*, (2002) **4**, No. 8, pp58-64.
- (7) 'Chemical and Physical Properties of Oil and Sand Solid', Chapter 2, in *Some Physical Properties of Bitumen and Oil Sand*, ed. by D. R. Prowse, Revision #2, Alberta Research Council Oil and Sands Research Department, Alberta, Canada (1983).

Table 1 Experimental Conditions of 3-D cell THAI/CAPRI Tests

Run	2000-07	2001-01
3-D Cell	0.6m × 0.4m × 0.1m	
Internal insulation	6 mm ceramic fiber layer	
Silicon Sand, W50, (kg)	34.1	29.09
Porosity (%)	39.05	
Gas permeability (mD)	1503	
Wolf Lake oil (kg)	6.90	
'Spiked' oil (kg)		5.63
Water (kg)		1.48
Synthetic Brine (kg)	1.74	
Na (ppm)	7,474	
Ca (ppm)	140	
Mg (ppm)	73.5	
Cl (ppm)	11,506	
SO ₄ (ppm)	560	
HCO ₃ (ppm)	254	
Total Salt (ppm)	20,007	
Catalyst (CoMo HDS)	Regenerated, 1/16" extrudate	
Catalyst loading (g)	191.1	172.5
Catalyst length (m)	0.3	
Well configuration	2VIHP	
Ignition	Hot Nitrogen	
Air flux (Sm ³ /m ² h)	15	
Initial sandpack temp. (°C)	20	
Back pressure (psig)	20 - 25	

Table 2 Tracers used in Run 2001-01

Standards		ρ g/ml	Amount		
			g	moles	ppm
undecane	n-C ₁₁	0.74	2.1	0.013	282
1-phenylhexane	C ₁₂ H ₁₈	0.86	4.2	0.026	570
perhydrofluorene	tricyc-C ₁₃	0.92	2.1	0.012	282
9,10-dimethyl anthracene	C ₁₆ H ₁₄	1.10	1.9	0.009	265
4,6-dimethyl dibenzothiophene	C ₁₄ H ₁₂ S	1.20	2.1	0.010	282
1-phenyldecane	C ₁₆ H ₂₆	0.86	2.3	0.011	315
3-decylthiophene	C ₁₄ H ₂₄ S	0.91	2.0	0.009	277
eicosane	n-C ₂₀	0.78	2.1	0.007	282
cholestane	tetracyc-C ₄₈	1.49	2.1	0.006	282
squalane	i-C ₃₀	0.86	4.2	0.010	565
Synthetic Crude Standard		0.88	25		3401
DILUANTS			29	ml	
hexadecane	n-C ₁₂		5	ml	
dodecane	n-C ₁₆		65	ml	
1-phenyltridecane	C ₁₉ H ₃₂		40	ml	
Total Mixture (liq at 50°C)			139	ml	

ρ -Density

**Table 3 Results of THAI/CAPRI Tests
(Wolf Lake Heavy Oil, 10.5 °API)**

Run	2000-07	2001-01
Recovery method	Primary	
Combustion mode	Dry and Wet	
Overall period (hr)	12.25	12
Pre-ignition period (hr)	2.25	2.25
Air injection period (hr)	10.0	9.75
Dry phase (hr)	7.0	6.75
Wet phase (hr)	3.0	3.0
Normal water injection (hr)	1.5	3.0
WOR (m ³ /1000Sm ³)	0.3	0.3
Air injection rate (l/min)	10	
Peak temperature (°C)	500-600	
Produced gas composition (% average)		
CO ₂	14.56	15.38
CO	4.88	5.49
O ₂	3.25	3.88
CO/(CO+CO ₂)	0.251	0.263
H/C ratio	0.05	0.0
O ₂ utilisation (%)	84.5	81.5
Furn consumption (%OOIP)	7.7	9.6
Oil Recovery (%OOIP)	87.1	82.0
Residual oil (%OOIP)	2.9	5.39
AOR (Sm ³ /m ³)	1130	1070
Combustion front velocity (m/hr)	0.05	0.05

Table 4 Elemental Analysis of Produced Oil (Run 2001-01)

Sampling time (min)		%C	%H	%O	%N	%S
0		83.89	10.74	1.07	0.41	4.86
20		76.28	11.38	7.84	0.37	4.50
65		76.38	10.47	7.54	0.36	4.39
123	Wet	71.41	10.95	12.75	0.30	3.73
180	THAI	60.04	11.06	21.37	0.22	2.99
209	CAPRI	75.56	12.45	6.73	0.22	3.18
356		85.27	11.23	0.83	0.08	2.97
389		84.73	12.60	1.08	0.07	3.05
453	Wet	84.56	10.59	0.76	0.13	3.41
512		84.57	10.59	0.74	0.13	3.46
>512		84.17	11.56	0.68	0.15	3.47

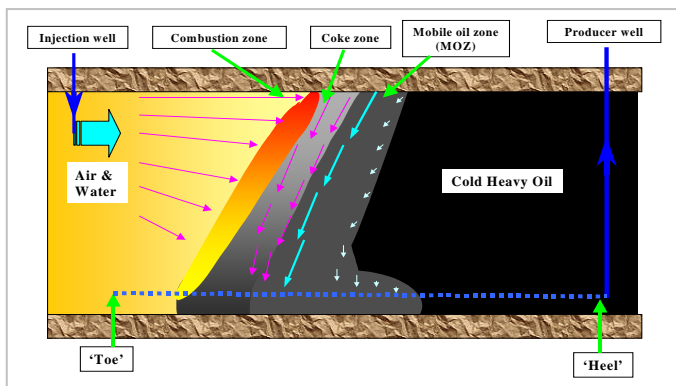


Figure 1. THAI – ‘Toe-to-Heel Air Injection’ Process

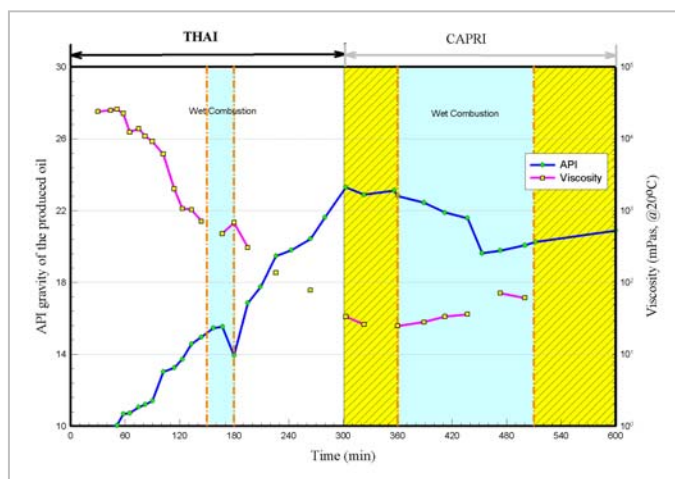


Figure 4. In situ upgrading of produced oil (Run 2001-01)

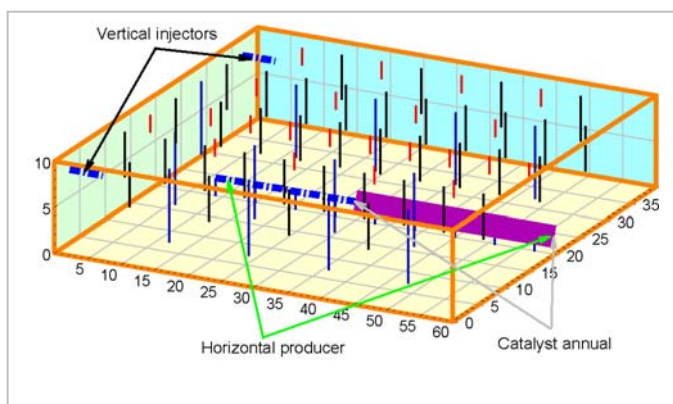


Figure 2. 3-D Combustion cell for the THAI/CAPRI tests

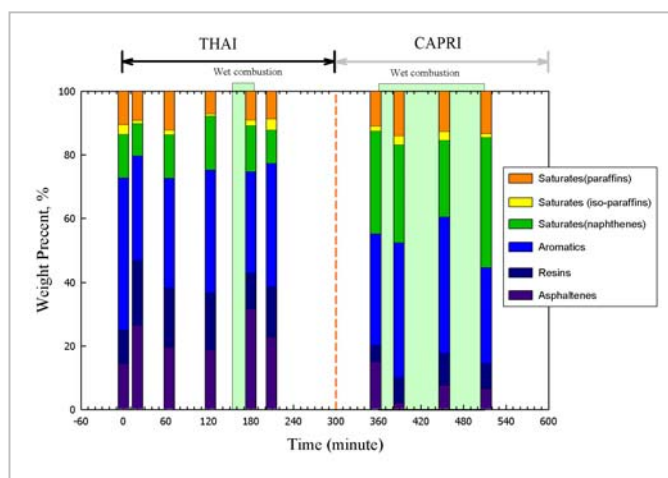


Figure 5. SARA/PIN analysis of produced oil (Run 2001-01)

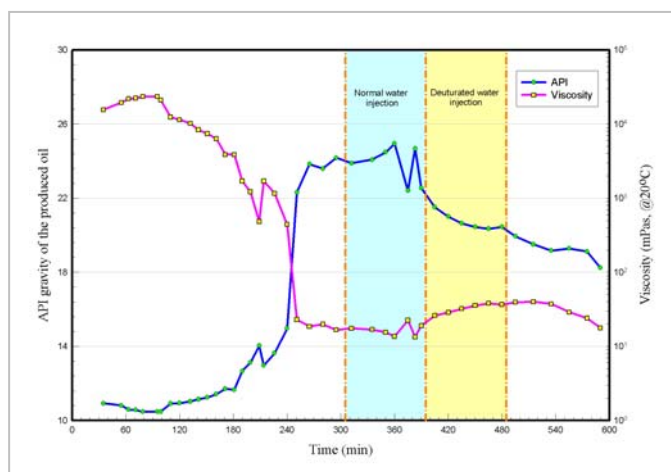


Figure 3. In situ upgrading of produced oil (Run 2000-07)

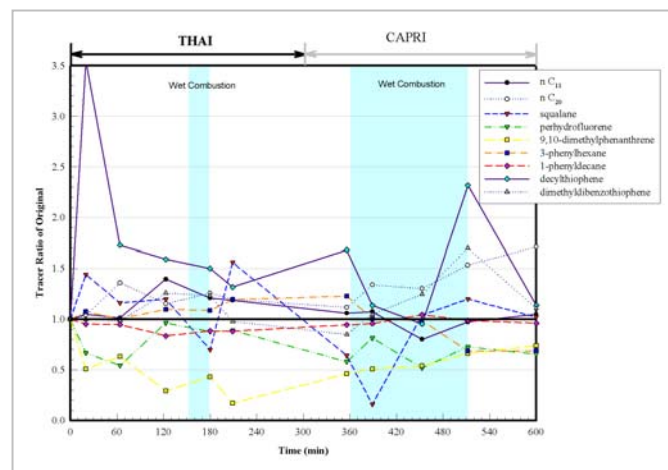


Figure 6. Tracer compounds in produced oil (Run 2001-01)

THE WRITE PROCESS FOR PRODUCING PIPELINEABLE HEAVY OIL

PART I: OPTIMIZATION OF THE DISTILLATE RECOVERY UNIT

Lee E. Brecher

Western Research Institute (WRI), 3474 North Third Street, Laramie,
Wyoming 82070

Abstract

The WRI Thermal Enhancement (WRITE) process is a field deployed bitumen upgrader capable of converting non-upgraded bitumen (as produced by in-situ production processes) into a residuum free heavy oil whose density and viscosity exceed the specifications for Canadian pipelines without the need for costly diluent additions. The WRITE process proceeds in two stages. The first is a low temperature thermal separation designed to remove distillate from the incoming stream and recover it as usable product suitable for blending with virgin oil or with overhead from the second stage. The heavy material not recovered from the distillate recovery unit flows to the continuous coker from which there is produced gas, a lighter cracked oil that is recovered as an overhead product and coke.

Process optimization begins with the distillate recovery unit (DRU) where the yield and quality of the oil recovered depend upon temperature, residence time, sweep gas composition and volume, and the nature of the incoming oil. The DRU optimization program seeks to understand each of these effects and to use that understanding in order to optimize the yield and quality of oil produced in the DRU.

Introduction

In addition to converting bitumen into a residuum free heavy oil whose density and viscosity exceed the specifications for Canadian pipelines, the process also produces sufficient quantities of coke to meet both its own thermal energy needs and also those of the production process as well. The bottomless heavy oil produced by the process may be transported to any refinery accessible to Canadian crude oils for further upgrading into finished products. The producer using the WRITE process is thus freed from the constraints imposed by diluent addition, has a reduced need for natural gas, and produces a product acceptable to any refinery or upgrader accessible to Canadian crude oils. This leads to four significant advantages for the producer:

(1) Each pound of non-upgraded bitumen fed to the process produces 0.6 to 0.8 pounds of residuum-free heavy oil that meets the Canadian pipeline specifications for density and viscosity and thus may be transported without diluent. Total flow per barrel of product is reduced by 50% or more from the production area and no diluent return lines are needed.

(2) The product crude is residuum-free and may be processed further in conventional upgraders to produce 30 to 40EAPI syncrude or it may be processed in refineries to finished products. The fact that the product contains no residuum removes the restriction that it be processed at a facility with a coker.

(3) After startup, approximately 75 pounds of coke are produced per barrel of process feed. This material has a heating value of around 15,000 Btu per pound and is sufficient not only for process needs but can also be used for the generation of production steam and

offsite needs. The small quantities of gas produced can be recovered and reformed to provide process hydrogen if needed.

(4) The flash and distillate recovery units are designed to accommodate feeds with up to 10% BS&W. As a result, minimal feed pretreating and conditioning is required. Similarly, the system is capable of continuously coking the bottoms from the distillate recovery unit. The large, semi-batch equipment characteristic of that used in delayed coking is unnecessary. System modularity with regard to the distillate recovery unit and the coker allow maximum flexibility for integration of the upgrading equipment with the production facility.

Experimental

Cold Lake crude received from Alberta Energy Company (now EnCana) was used as the starting feed in all of the optimization studies. This oil was processed in the one-barrel-per-day DRU located at WRI's Advanced Technology Center (1) at stage temperatures of up to 700°F. The bottoms from each of these runs were processed further in the 6-inch rotary screw coker to produce light, cracked overhead product for blending with the corresponding DRU overheads. DRU yields as a function of stage temperature are shown in Figure 1 and selected DRU overhead properties are shown in Figure 2. Storage stability of the liquid products was performed according to ASTM D4625 and the compatibility tests were carried out according to a test developed by Wiehe (2). Products from processing Athabasca bitumen in the WRITE process have been shown to be relatively stable during 4 weeks storage at 43°C, in spite of having high olefinic content. Furthermore, the distillate products are compatible with most Alberta crude oils (3).

Results and Discussion

Four levels of processing severity are being investigated in the DRU optimization study and the results of these tests are summarized in Figure 1. The first level of processing severity involves normal distillation (the NBP curve used in the NCUT economic evaluation) and produces DRU overhead yields approaching 25% as the stage temperature approaches 750°F. Increasing the processing severity slightly, as was done in the stability and compatibility study (2), enables yields of >30% to be achieved at temperatures below 700°F, while moderate increases in severity enable these results to be extended to yields exceeding 40% at temperatures below 675°F. A new series of experiments is presently being planned with the objective of achieving DRU yields in excess of 45% while maintaining temperature below 650°F.

An examination of Figure 2 shows no perceptible changes occurring in overhead product quality, at least not as measured by API gravity, as processing severity is increased. Quite the contrary situation exists with the DRU bottoms, however, as the density of this oil shows marked increases with increasing processing severity.

Conclusions

These activities have confirmed that as-produced, non-upgraded bitumen from Canadian oil sands can be converted continuously into residuum-free, synthetic heavy oil, along with associated quantities of gas and coke. The naphtha fraction of the produced oil comprises about 6% by weight of the total oil and contains olefins and diolefins that will have to be hydrotreated before its addition to the pipeline. The remainder of the oil, comprising about 67% by weight of the total oil fed, has a density and a viscosity compatible with

specifications governing Canadian pipelines and can be admitted without the need for diluent. Stability and compatibility testing on this oil has shown it to be stable and compatible with other common Albertan crude oils. Energy for the process is available in the coke produced as a process by-product and the gases produced contain sufficient hydrogen to stabilize the naphtha fraction. Processing conditions are mild, do not involve the use of excessive temperatures or pressures and allow the presence of BS&W in the feed oil.

Acknowledgements. This project was funded by the US Department Energy (USDOE) under Cooperative Agreement No. DE-FC26-98FT40322. This support is gratefully acknowledged.)

Disclaimer

This report was prepared as an account of work sponsored in part by an agency of the United States Government. Neither the United States Government nor any agency thereof, nor any of their employees, makes any warranty, expressed or implied, or assumes any legal liability or responsibility for the accuracy, completeness, or usefulness of any information, apparatus, product, or process disclosed, or represents that its use would not infringe privately owned rights. Reference herein to any specific commercial product, process, or service by trade name, trademark, manufacturer, or otherwise, does not necessarily constitute or imply its endorsement, recommendation, or favoring by the United States Government or any agency thereof. The views and opinions of authors expressed herein do not necessarily state or reflect those of the United States Government or any agency thereof.

References

- 1- Brecher, Lee E., "The Use of TaBoRR as a Heavy Oil Upgrader", Presented at the 20th Annual Pacific Coast Oil Show & Conference, Kern County Fairgrounds, Bakersfield, November **2001**
- 2- Parviz Rahimi, Lee E. Brecher and Theo deBruijn, "Stability and compatibility of liquid products obtained from cold lake bitumen using the WRITE process", Presented at the 8th International conference on stability and handling of liquid fuels, Steamboat Springs, Colorado September 14-19, **2003**
- 3- Brecher, Lee E., Rahimi, P, deBruijn, T and Flaherty, G., "Preliminary assessment of the TABORR process and the stability and compatibility of its products", Presented at the Petroleum Chemistry Division, 225th ACS National Meeting, New Orleans, LA, March 23-27, **2003**
- 4- Parviz M. Rahimi, Jinwen Chen, Lee Brecher and Theo deBruijn, "Hydrotreating of liquid products from cold lake bitumen obtained in the WRITE process", Presented at the Division of Fuel Chemistry, 227th ACS National Meeting, Anaheim, CA, March 28-April 1, **2004**

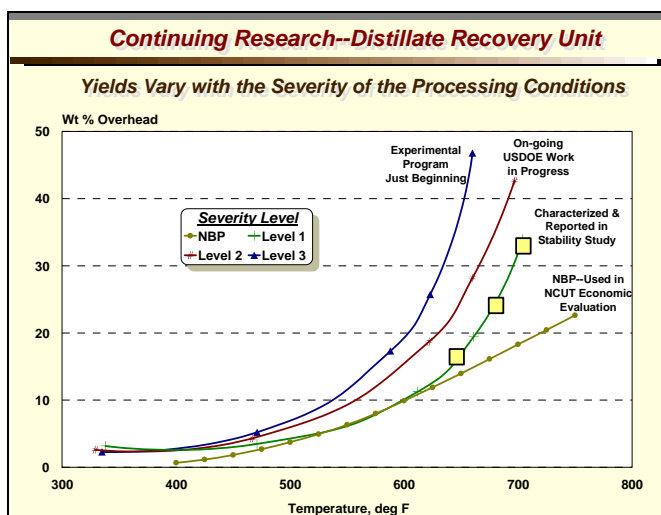


Figure 1. DRU yields as a function of stage temperature

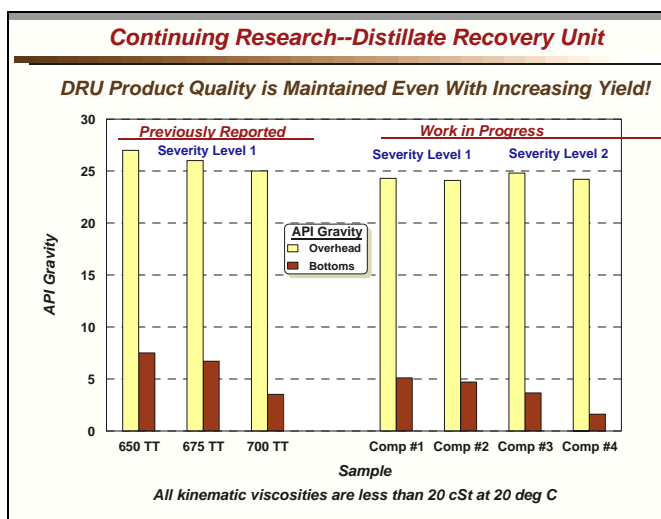


Figure 2. Selected DRU overhead properties

HYDROTREATING OF LIQUID PRODUCTS FROM COLD LAKE BITUMEN OBTAINED IN THE WRITE PROCESS

Parviz M. Rahimi¹, Jinwen Chen¹, Lee Brecher² and Theo deBruijn¹

¹National Centre for Upgrading Technology (NCUT), 1 Oil Patch Drive, Suite A202, Devon, Alberta T9G 1A8 Canada

²Western Research Institute 3474 North Third Street, Laramie, Wyoming 82070

Abstract

The WRITE process is a new emerging thermal cracking technology for the conversion of heavy oils and bitumen to synthetic crudes. The distillate products of any thermal bitumen processing, including the WRITE process, contain unsaturated compounds such as olefins and di-olefins. It is desirable to remove or convert these materials to saturated compounds before they reach refineries for processing. Hydrotreating of WRITE distillate products (-250°C) containing a significant amount of olefins and di-olefins was performed in a batch autoclave using spent commercial NiMo/Al₂O₃ hydrotreating catalyst. It was shown that at relatively mild conditions all di-olefins were converted to olefins or saturated compounds, but conversion of olefins required higher severity. Hydrotreating reactivity of WRITE products was compared with that of coker naphtha.

Introduction

When heavy hydrocarbons such as bitumen are subjected to thermal treatment for the production of synthetic crude, in the absence of hydrogen (to cap the intermediate free radicals) a significant amount of olefins and di-olefins are formed through free radical disproportionation reactions. The analytical procedures such as FIA and bromine number, developed for the determination of the olefin content for refinery products, are not suitable for crudes. In both of these methods components such as aromatics interfere with analyses, resulting in erroneous results.

Most existing and emerging upgrading technologies for conversion of heavy oils and bitumen to transportation fuels are based on thermal processes like visbreaking, coking and pyrolysis. These processes are performed in the absence of catalysts and hydrogen where a significant amount of unsaturated products are produced. Among those unsaturated compounds there are products such as conjugated di-olefins that are very reactive and can polymerize and form coke in different parts of a refinery. Although compounds with isolated olefinic bonds form in higher concentration than di-olefins during thermal reaction, they are less reactive. In the presence of oxygen, olefins can form hydroperoxide and initiate a free radical chain reaction. Due to their high reactivity, these materials can form sediment and sludge during fuel storage and the refining processes.

The WRITE process (Western Research Institute Thermal Enhancement) is a new thermal process for heavy oil conversion that is currently under review by a number of producers in Alberta. It is expected that the liquid products from this process will contain some olefins and di-olefins. The presence of these unsaturated materials in synthetic crudes has raised some concerns related to their stability during storage, pipelining and subsequent processing in refineries. The pipeline specification for the olefin content in crude is set by CAPP (Canadian Association for Petroleum Producers) at <1% by volume. Another pipeline specification, which is indirectly related to the olefin content of crude, is based on the bromine number of the -250°C cut and is set at <10 gBr₂/100g.

The objectives of this preliminary research are: 1) to investigate hydroprocessing conditions at which the -250°C distillate fraction products obtained from Cold Lake bitumen in the WRITE process meet pipeline specifications for bromine number (<10 gBr₂/100g); 2) to compare hydrotreating reactivity of the -250°C distillate fraction from the WRITE process with fluid coker naphtha at the same reaction severity.

Experimental. Hydrotreating experiments were carried out in a 300 mL stirred tank autoclave equipped with a catalyst basket. In a typical experiment, about 104 g of feed (coker naphtha or WRITE -250°C distillate fraction) was placed in the reactor. A spent commercial NiMo/Al₂O₃ hydrotreating catalyst (18.6 g) was used in all experiments. The reaction temperature and hydrogen partial pressure used in these experiments are shown in Table 1. When the internal temperature of the autoclave was 5°C below the set point, the yield period time was begun. The autoclave furnace was turned off 60 minutes from this time. After the reactor cooled down to room temperature, the gas contents of the autoclave transferred to a gasbag; the gas volume in the bag was measured and the content was analysed by gas chromatography. The reactor was opened and the liquid contents were removed and analyzed for bromine number and diene content (UOP-326-82).

Results and Discussions

The WRITE process is a new thermal processing technology that is currently being considered for the conversion of bitumen from oil sands to liquid fuels (1). Products from processing Athabasca bitumen, in the WRITE process, were shown to be relatively stable during 4 weeks storage at 43°C, in spite of having high olefinic content. Furthermore, the distillate products were compatible with most Alberta crudes (2). The refiners wish to receive feedstocks with no olefins or di-olefins content and discount streams that are high in such components. There are two options for removing unsaturated compounds from petroleum feedstocks. Olefinic compounds can be either extracted and used as petrochemical feedstock (3) or hydrotreated to form stable hydrocarbons.

In the present work it was decided to investigate the feasibility of hydrotreating the WRITE distillates (-250°C fraction) to produce products that were acceptable by refineries in terms of the olefin and di-olefin contents. Since a limited quantity of WRITE product was available, only a series of batch autoclave hydrotreating runs were performed to investigate the optimum conditions for the removal of olefins and di-olefins. We plan to carry out an extensive hydrotreating study using bench-scale continuous operation when larger quantities of distillates are available. For the purposes of comparison with the hydrotreating reactivity of the WRITE liquid products, we also selected a fluid coker naphtha and performed hydrotreating with the same catalyst and under similar reaction conditions.

Analysis of feedstocks and hydrotreated products from the coker naphtha and the WRITE feedstock (-250°C fraction) are shown in Table 1. Two analytical tests, namely diene number (UOP-326-82) and bromine number (ASTM D-874), were used to determine the degree of saturation of the unsaturated compounds after hydrotreatment. In the absence of more accurate analytical methods for quantitative determination of unsaturated compounds (olefins and di-olefins), we used the existing analytical methods to follow the directional changes in the properties of the distillate as a function of hydrotreating severity.

The analysis shown in Table 1 indicates that the coker naphtha had higher diene as well as higher bromine numbers compared to the WRITE feed.

The higher reactivity of dienes compared to olefins is clear for both feedstocks as these materials are converted to olefinic or saturated compounds at the lowest hydrotreating severity employed. The diene concentration in coker naphtha changed from 13.9 gI₂/100g in the feed to 0.5 gI₂/100g in the product at a reaction temperature of 200°C. Similar results were obtained in hydrotreating the WRITE feed. The diene concentration changed from 4.2 gI₂/100g in the feed to 0.0 gI₂/100g in the hydrotreated products at the same reaction temperature. The conversion of isolated olefinic double bonds to saturated compounds required higher temperature and hydrogen pressure compared to the dienes conversion. The data in Table 1 also show that at lower reaction severity the saturation of olefinic compounds in the coker naphtha, as determined by bromine numbers, is faster than that in the WRITE feed. However, at higher reaction severity olefins in the WRITE feed are hydrogenated faster than those in coker naphtha.

Table 1. Properties of Feedstocks and Hydrotreating Products

Feed	Temp. and H ₂ Partial P	Diene gI ₂ /100g	Bromine # gBr ₂ /100g
Coker Naphtha feed		13.9	84.2
WRITE feed		4.2	53.3
Coker Naphtha	200°C/500psi	0.5	76.7
WRITE feed	200°C/500psi	0.0	50.0
Coker Naphtha	300°C/700psi	0.07	50.8
WRITE feed	300°C/700psi	0.0	27.4
Coker Naphtha	350°C/1000psi	0.3	19.7
WRITE feed	350°C/1000psi	0.0	9.0

Conclusions

This study demonstrated that it is possible to convert olefins and di-olefins, produced during the thermal reaction of Athabasca bitumen in the WRITE process, by mild hydrotreating. It was shown that the hydrotreating reactivity of WRITE distillates (-250°C) was comparable to that of fluid coker naphtha.

Acknowledgement. This project was funded by WRI through the US Department Energy (USDOE). Partial funding for NCUT has been provided by the Canadian Program for Energy Research and Development (PERD), the Alberta Research Council (ARC) and the Alberta Energy Research Institute (AERI).

References

- 1- Brecher, Lee E., Rahimi, P., deBruijn, T and Flaherty, G., "Preliminary assessment of the TABORR process and the stability and compatibility of its products", Presented at the Petroleum Chemistry Division, 225th ACS National Meeting, New Orleans, LA, March 23-27, **2003**
- 2- Parviz Rahimi, Lee E. Brecher and Theo deBruijn, "Stability and compatibility of liquid products obtained from cold lake bitumen using the write process", Presented at the 8th International conference on stability and handling of liquid fuels, Steamboat Springs, Colorado September 14-19, **2003**
- 3- Sharma, Y.K., Reimert, R, and Singh, I.D. "Stabilization studies of middle distillate fuels: Structural composition of insoluble by FTIR spectroscopy", *Petroleum Science and Technology*, 21, 7-8, 1055-1063, **2003**

IMPROVED MOLIBDENUM SULPHIDE NANODISPERSED CATALYST FOR HYDRO PROCESSING, PREPARED VIA MICROEMULSIONS

Emir Escalona², Rebecca Wang¹, Carlos Scott², Josephine Hill¹,
Pedro R. Pereira-Almao¹

¹Department of Chemical and petroleum Engineering, University of Calgary, 2500 University Drive, NW, Calgary, Alberta, Canada

²Centro de Catalisis, Petroleo y Petroquimica, Escuela de Quimica, facultad de Ciencias, Universidad Central de Venezuela. Los Chaguaramos, Caracas, Venezuela

Introduction

Due to environmental restrictions as well as to limitations of performance of traditional fixed bed catalysts for hydro processing extra heavy feedstocks, the generation of micro-nano size catalyst particles within the feed at conditions close to the ones available in the reaction zone is an important alternative. It has allowed the proposition of a set of many different new processes that could be considered the third generation hydro processing of residues and bitumen.

Oil soluble compounds of those transition metals catalytically active for hydro processing yield very good results [1] but their preparation is expensive. Most of the inorganic forms of these transition metals are much less expensive, for instance, ammonium heptamolibdate is perhaps the least expensive form of Mo with the highest metal proportion within the salt. Nevertheless its insolubility in the reaction media prevents from obtaining a good dispersion of the metal, which makes necessary to incorporate significant amounts of the compound to get sufficient catalysis.

Traditionally more considered for heavy crude oils transporting [2] the use of emulsions and micro emulsions are an alternative way of incorporating well dispersed catalysts for heavy feedstocks hydro processing. In this paper the preparation of micro/nano dispersed Mo particles by thermal decomposition of ammonium heptamolibdate emulsions was studied. The effects of nature and quantity of pre-sulphuring agents dissolved in the emulsion as well as the effect of surfactant were some of the variables determined by using a Design of Experiment method.

Experimental

Emulsions preparation

1-metilnaphthalene (1-MN), an oil lubricant base and a Light Vacuum Gas oil were all used as different oil basis for the preparation of the emulsions. The aqueous phase was prepared containing ammonium heptamolibdate (7.5% Mo) with or without ammonium sulphide at two different concentrations (3 and 10%). Also different percentages of surfactant were used from 1 to 10%.

Thermal decomposition of the emulsions

The emulsions were decomposed in two different reactor set-ups, an autoclave reactor and a continuous reactor, in a temperature range between 200 and 300C at either atmospheric pressure or at 1000 psig., In the case of using autoclave a mechanical stirring was set at 300 rpm. In the autoclave the emulsion was entered into the reactor once the temperature and pressure conditions were reached. After 5 minutes, the thermally decomposed solid is recovered by centrifuging, washing several times with toluene and dried at 125C during 4 hours.

Solids Characterization

X Ray Photoelectron spectroscopy (XPS)

A Leybold-Heraeus equipment model LH-11 was used. The radiation was provided with an Al anode (1486.6 eV) and a power of 350 watts. Pass energy at 50 eV. The C_{1s} line (284.6 eV) was used as reference for calibration of Binding Energies (BE) for the different elements as well as for charge effects correction.

X Ray Diffraction (XRD)

A diffractometer DRX Philips model PW3710 at powder was used, employing a graphite monochromator. An APD program from Phillips was used for detection and recording. A scintillate detector was used. Continuous scan of the diffraction angles was performed from 5.00 until 75.69° (2θ). A Cu anode Kα1 emission line was used.

Surface area

The samples were pretreated in a degasifier VacPrep 061 from Micromeritics at 120°C, desorbed under vacuum (1×10⁻⁴ torr) for 2 hours. Specific surface area is determined by adsorption-desorption of nitrogen following the standard BET method. The microporous volume was determined with the t method, the pore radii distribution by the method of Roberts with the cylinder pores model. Additionally a pore distribution was performed on some solids using the BJH method (Barret, Joyner, Hallenda).

Results and Discussion

In figure 1 are shown the XRD analysis of some solids prepared by thermal decomposition of the emulsions prepared using 1-Methyl Naphthalene as the oil phase. It can be observed that these solids are poorly crystallized showing a pattern of amorphous Molybdenum Disulfide. The main reflections observed are the ones corresponding to the faces 002, 100, 103 and 110. Nevertheless, differences are perceived regarding the intensities of the reflections in particular that of the face 002. Based on the intensities of the face 002, the solids obtained from the decomposition of emulsions containing 3% ammonium sulphide were the ones showing higher piling. It seems that the use of a higher proportion of ammonium sulphide decreases the piling. In addition, the use of higher proportions of surfactant also resulted in reduced ray intensities particularly in the phase 002. Apparently a lower drop size in the emulsion conduces to a lower extent of crystals growing and to a higher disorder of lamellas when the progression is done from macro emulsions (1% surfactant) toward micro emulsions(10%).

In figure 2, are shown the XPS spectra obtained for the solids prepared via flashing and decomposition of the emulsions. The signal centred at 226.3 eV is assigned to the binding energy of the sulphur 2s orbital. As observed each spectrum is the result of the overlapping of signals corresponding to the principal oxidation states of Mo, which are centred at 229.1 and 232.3 eV, representing the doublets 3d, 3d_{5/2} and 3d_{3/2}. These results suggest that Mo is mostly present under the oxidation state +4, even though the intensities do not correspond with the existence of a unique oxidation state.

In table 1 the BET areas of some of the solids obtained and their corresponding catalytic activity for the hydrodesulphurisation of Thiophene are presented. The solids prepared with the higher proportion of surfactant, which implies lower drop size (micro emulsions) present higher surface area as well as much higher catalytic activity for the desulphurisation of Thiophene.

The results presented were very similar to the ones obtained by preparation of the ultra dispersed solids in a continuous decomposition set-up, in which the conditions were implemented to produce nano particles of both Mo oxide as well as Mo Sulphide.

This second solid was also obtained by incorporating to the aqueous Mo solution different proportions of ammonium sulphide. Thus the pre-sulphuring at an early emulsion preparation stage eliminates the need for addition of pre-sulphuring agents as required when Mo oxide is first obtained.

Reduced nano particle size, increased disordered lamellar nano particles and consequently enhanced catalytic activity were obtained by this continuous method which simulates at lab scale a real on line incorporation of the catalyst occurring in a slurry type hydro conversion processing of hydrocarbon residues.

Conclusions

Nano particles of Mo oxide and Mo sulphide were produced via thermal decomposition of emulsions and micro emulsions containing Mo Heptamolibdate in the aqueous phase by using both a batch and a continuous reaction set-up. The solids obtained presented differences in the pre-sulphuring level due to the proportions of ammonium sulphide incorporated to the aqueous solutions. The solid produced from micro emulsions, prepared with increased amounts of surfactants were found the more dispersed and active toward the Thiophene HDS reaction test. No significant differences were found for the two different preparation set-ups employed.

References

- [1] *Bearden R., Aldridge C. L.*, *Energie Progress*, **1** (1981) 44.
 [2] *Ng F.T.T. Rintjema R.T.* *Stud. Surf. Sci. Catal.*, **73** (1992) 51.

Acknowledgment

Emir Escalona, first author of this work, was partly supported by PDVSA-INTEVEP and the batch experiments were done at that site in Los Teques, Venezuela.

Table 1. BET Area and Catalytic Activity

Sample	Area (m ² /g.)	Rel.Activity
3%(NH ₄) ₂ S/1%Surf.	3	1
10%(NH ₄) ₂ S/1%Surf.	5	4
10%(NH ₄) ₂ S/5%Surf.	10	49
10%(NH ₄) ₂ S/10%Surf.	38	54

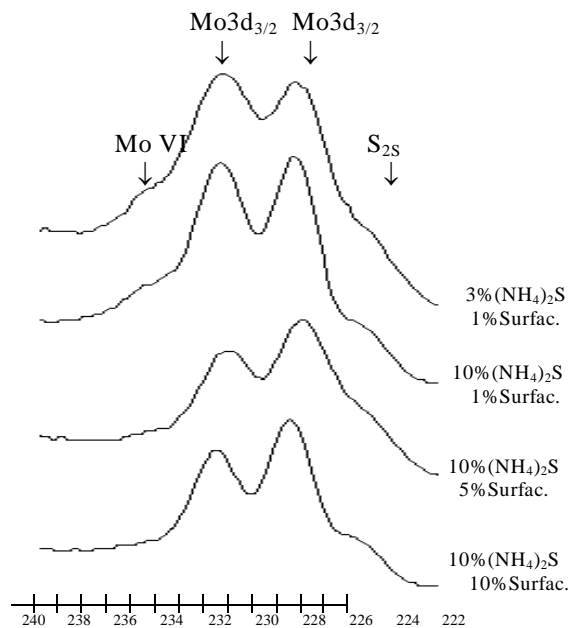


Figure 2. XPS spectra of the different solids.

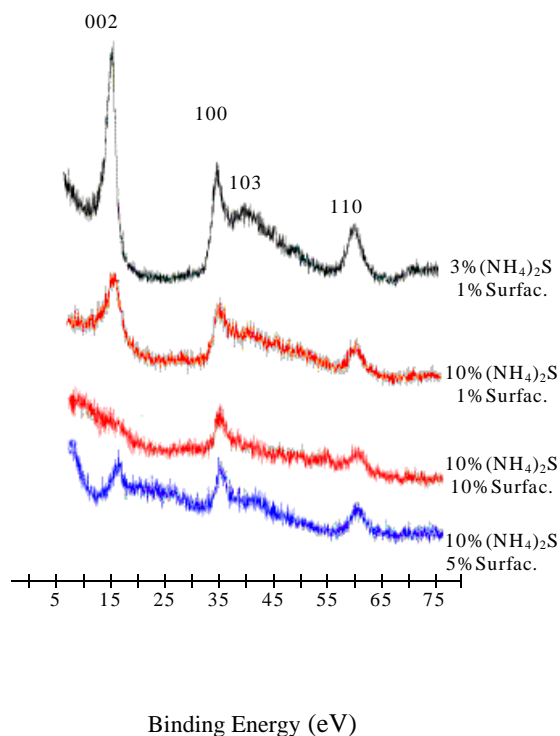


Figure 1. Diffractograms of different solids prepared

REMOVAL OF NICKEL AND VANADIUM FROM HEAVY CRUDE OILS BY EXCHANGE REACTIONS

John G. Reynolds

Forensic Science Center
University of California
Lawrence Livermore National Laboratory
P. O. Box 808, L-178
Livermore, CA 94551

Introduction

Current Methods of Heavy Crude Oil Processing. The upgrading of heavy crude oil occurs generally by either hydrogen addition- or carbon rejection-type processes¹. Hydrotreating is attractive because US refineries have moderately high capacity, but it is costly because it requires added hydrogen, requires appropriate metallurgy to handle the severity of conditions (high temperature and pressure), and, because of poor catalyst lifetimes (because of high metals in heavy crude oils), has high catalyst costs and non-productive downtime. In addition, with heavy crude oils, boiling point reduction is necessary for conversion to transportation fuels, so an additional cracking step is required.

Hydroconversion circumvents this cracking problem. However, similar problems to hydrotreating are encountered, such as hydrogen and metallurgy costs, with the additional problems of technology development (just beginning to become commercially available), and capital equipment investment.

Fluidized cat cracking (FCC) is also attractive because US refineries have very high capacity. Process wise, it is ideal because of the cracking step necessary to produce light components. However, FCC catalysts are notoriously metals intolerant (although new generations of RFCC catalysts show some promise), and with high S and N contents of heavy feeds, high SO_x and NO_x emissions during catalyst regeneration can be costly to abate.

Coking is also an attractive upgrading method for heavy crude oils. The US has very high capacity and more units are relatively cheap to build because severe-service metallurgy is not required. The drawbacks include poor quality products such as coke and coker gas oils, and fairly large yield losses due to the carbon rejection through coke.

Pretreatment of Heavy Crude Oils to Remove Metals. The high metals levels of heavy crude oils currently necessitate the processing to be costly, either through the high costs of hydrogen addition or high yield loss due to carbon rejection. If metals could be removed in a pretreatment step before the heavy crude oil enters processing streams, then heavy crude oils could be more cost effectively processed by traditional methods. Hydrotreating could be utilized to a greater extent to remove the high S and N levels (for which the catalysts are specifically designed) without the quick deactivation by metals poisoning. Very-active zeolites could be used in FCC for the extensive cracking needed for boiling point reduction, and coking could be used less because the other processes could be used more, therefore avoiding such high carbon yield losses to coking. Hydroconversion units may not have to be built avoiding high capital expenditure.

The approach to the pretreatment step for metals removal can be by various methods. In this report, surrogate metal solutions containing the metal bound as petroporphyrin, or petroporphyrin fractions isolated from heavy crude oils are treated with a variety of chemical agents, and then washed with aqueous solutions to remove the metals.

Experimental

Reagents. Ethylenediamine tetraacetic acid (EDTA) •2H₂O was purchased from Sigma; disodium salt of EDTA (Na₂EDTA), nitrilotriacetic acid (NTA), disodium NTA (Na₂NTA), diethylenetriamine pentaacetic acid (DEPTA), N-(2-hydroxyethyl)ethylene diamine triacetic acid (N-HEEDTA), trisodium N-HEEDATA (Na₃N-HEEDTA), benzoic acid, malic acid, malonic acid, maleic acid, maleic anhydride, fumaric acid, oxalic acid, triethylcitrate, hexamethylenetetraamine (HMTA), phthalocyanine, tetraphenyl porphyrin, catechol, di-*t*-butyl catechol, coumarin, formic acid, diethyldithiocarbamate sodium salt (Et₂dtcNa)(H₂O)₃, Et₂dtc diethylammonium salt (Et₂dtcEt₂NH₂), *t*-butyl hydroperoxide, cumene hydroperoxide, peroxyacetic acid, sodium sulfide nonahydrate (Na₂S•9H₂O), Fuller's Earth, bentonite, montmorillonite, pyridine-N-oxide, 3-pyridylcarbinol-N-oxide, acetone oxime, titanium tetrakis-*i*-propoxide (Ti(OCH(CH₃)₂)₄), titanium oxide acetyl acetonate (TiO(acac)₂), fluorosulfonic acid (FSO₃H), trifluoro sulfonic acid (CF₃SO₃H), DMF, and 1-MN were purchased from Aldrich Chemical Co; tartaric acid was purchased from Baker Chemical Co.; CH₂Cl₂, toluene, and methanol were purchased from Baxter Scientific; DMF was purchased from EM Scientific; carbon dioxide, carbon monoxide, oxygen were purchased from Matheson; titanium dioxide (TiO₂), was purchased from Allied Chemical Co; VO(etio) and Ni(etio), were purchased from Midcentury Chemical Co., Posen, IL. 1,4,8,11-tetraazacyclotetradecane (Cyclam) was prepared by the method of Richman and Atkins².

Reactions. The following is a typical reaction mixture (weights and volumes were chosen to give 10 to 200 ppm by weight porphyrin solutions which were easy to monitor by UV-vis spectroscopy): 0.0024 g VO(etio) were dissolved in 20 ml of 1-MN, toluene, DMF, or CH₂Cl₂ and heated to the appropriate reaction temperature with a constant control heating mantle (J-KEM Scientific Model 210). The starting concentration was then determined by UV-vis spectroscopy. Approximately 0.04 ml (~ 100 mole equiv.) of the ligand or reagent were added. Aliquots of the reaction mixture were taken at various times to primarily monitor the disappearance-appearance of the porphyrin species.

Analyses. The fractions were examined for porphyrin content by UV-vis and second derivative UV-vis spectroscopy utilizing an HP 8452A diode array system. The spectra were collected as zero order using maximum integration time. Second derivative spectra were calculated after averaging. The entire fraction was dissolved in either CH₂Cl₂ or toluene. The amount of solvent was determined by diluting the sample so the spectral region less than 380 nm was on scale. This ranged from 25 to 100 ml in most cases.

Results and Discussion

Screening Studies. Most reagents were tested using vanadyl etio porphyrin (VO(etio)) and watching the characteristic UV-vis spectrum change. The most effective reagents were found to be maleic acid in dimethylformamide (DMF), montmorillonite in 1-methyl naphthalene (1-MN), CF₃SO₃H in 1-MN, and FSO₃H in 1-MN, with the fastest (maleic acid at 100 mole equivalents) completely reacting with VO(etio) in 10 min. or less.

These agents were found through the testing of many different types of chemical agents, having functional groups, chelating ability, and oxidation-reduction properties. Table 1 shows an example of test data using carboxylic acids and mixtures as the

reactants. The results for all materials used in the screening studies are summarized:

- Amino-carboxylate compounds: nitrilotriacetic acid works well in DMF
- Polyamino compounds: none
- Dithiocarbamates: none
- Carboxylic acid compounds: malic, benzoic, maleic, and malonic work well in DMF
- Clays: montmorillonite works well in 1-MN
- Catechol compounds: none
- Coumarin works well in DMF
- Amino-N-oxides: none
- S²⁻ does not work
- Hydroperoxides: *t*-butyl and cumene work well in DMF
- Peroxyacetic acid works very well in methylene chloride
- Oxo-titanium compounds: none
- Superacids: fluoro- and trifluoromethane sulfonic acids work well in 1-MN

Solvent effects were found for most agents tested also. Most exhibited some activity in DMF, while little or no activity in 1-MN. The agents tested in methylene chloride also generally showed excellent activity.

Table 1. Screening Studies on the Reactivity of Carboxylic Acids with VO(etio)

Reactant	Solvent System	Time Reacted	Temperature ° C	% P Removed
Tartaric	DMF	1.5 h	153	NR
Triethyl citrate	DMF	2 h	120	50
Triethyl citrate	<i>o</i> -xylene	3 h	142	NR
	<i>o</i> -xylene	18 h	142	NR
+ diethanol amine	1-MN	24 h	NA	NR
Succinic	1-MN	1 h	160	NR
	1-MN	2.5 h	222	NR
Malic	DMF	21 h	NA	99
+ quinoline	1-MN	24 h	189	18
Oxalic	DMF	24 h	153	NR
2-Ethylhexanoic	DMF	30 m	146	NR
+ air	DMF	1 h	130	NR
Fumaric	DMF	30 m	145	23
Benzoic	DMF	3.5 h	153	100
Benzoic	<i>o</i> -xylene	3 h	126	NR
	<i>o</i> -xylene	18 h	142	NR
+ HMTA	1-MN	8 h	184	28
+ diethanolamine	1-MN	24 h	NA	NR
Maleic	DMF	10 m	153	100
Maleic Anhydride	DMF	1 h	132	58
Malonic	DMF	24 h	153	100

HMTA = hexamethylenetetraamine

Superacid Reactions. A more detailed examination of the effectiveness of low concentrations of the superacids, fluorosulfonic acid (FSA) and trifluoromethane sulfonic acid (TFMSA), as demetallation agents for nickel and vanadium porphyrin compounds was conducted. Superacids were found to be extremely effective in demetallating vanadyl etio (VO(etio)) and nickel (Ni(etio)) etio porphyrin screening compounds as shown above. For examples, almost complete reaction was observed for VO(etio) in toluene at 72°C and 100 mole equivalents of TFMSA at 3 min. reaction time, while only 30% reaction was observed with CF₃COOH (another recognized strong acid) under similar conditions at 60 min. reaction

time. Figure 1 shows the test results for TFMSA at 200 mole equivalent.

The porphyrin fractions isolated from Hondo 650°F⁺ and Kern River 650°F⁺ residua took 600 mole equivalents and 45 min. at 79°C for essentially complete reaction. Only 60% reaction of the petroporphyrins could be attained using 600 mole equivalents at room temperature.

The mechanism of reaction appears to be dependent on the porphyrin species. The behavior of VO(etio) with TFMSA suggests an adduct-type compound is formed first which then goes on to form demetallated and other products. The adduct-type compound appears to regenerate VO(etio) upon reaction with acidic water. Ni(etio) and H₂etio were found to immediately produce the non-metallated porphyrin dication, H₄etio²⁺, with no evidence of unreacted porphyrin. The reaction of VO(TPP) with TFMSA exhibited evidence of the H₄TPP²⁺.

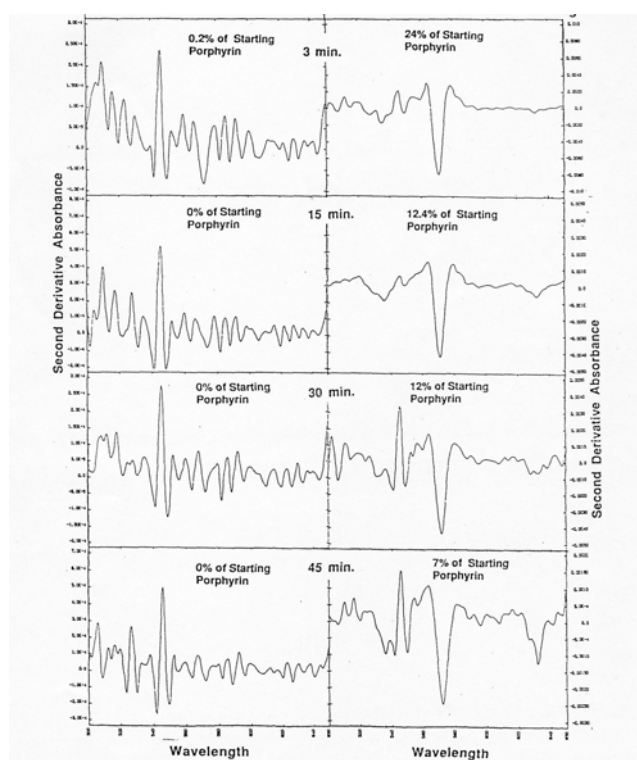


Figure 1. Second derivative UV-vis spectra of the reaction of VO(etio) porphyrin with 200 mole equivalents of TFMSA in toluene at 72°C. The y-axis is the second derivative relative absorbance. The Figures on the left side are the spectra after reaction and the figures on the right side are the corresponding spectra after water wash.

Acknowledgement. This work was funded through a CRADA between Phillips Petroleum Company and LLNL. This work was performed under the auspices of the U. S. Department of Energy by the University of California Lawrence Livermore National Laboratory under Contract No. W-7405-ENG-48.

References

1. Schuetze, B. and Hofmann, H., *Hydrocarbon Processing*, 1984, **63**(2), 75-82.
2. Richman, J. E., and Atkins, T. J., *J. Am. Chem. Soc.*, 1974, **96**(7), 2268-2270.

PREDICTION OF DENSITY AND CETANE NUMBER OF DIESEL FUEL FROM GC-FIMS AND PIONA HYDROCARBON COMPOSITION BY NEURAL NETWORK

Hong Yang, Yevgenia Briker, Renata Szykarczuk and Zbigniew Ring

The National Centre for Upgrading Technology, Devon, AB,
Canada, T9G 1A8

Introduction

Modeling and optimization of bitumen upgrading processes require reliable correlations to predict the key properties of the product stream based on its computer-generated composition. In the approach taken by the National Centre for Upgrading Technology (NCUT), these models are designed so that this computer-generated composition is equivalent to the various available chromatographic tests. This effectively decouples the development of the main parts of any process model: the reactor and product quality models. As part of its process modeling program, NCUT has assembled a large database of diesel fuels. The chemical compositions of the diesel fuels were characterized by several chromatographic methods. A neural network approach was then taken to correlate fuel properties such as density, aniline point, cloud point, viscosity, refractive index, molecular weight and cetane number with chemical compositions. This work presents the preliminary results on the correlation of density and cetane number with the hydrocarbon compositions of diesel fuels given by the sum of GC-FIMS (Gas Chromatograph-Field Ionization Mass Spectrometry) and PIONA results (normal paraffins, isoparaffins, olefins, naphthenes and aromatics).

Method

One hundred fourteen diesel samples were prepared by blending 15 original diesel components obtained from Canadian refineries and derived from both conventional crude oil and oil-sands bitumen. Cetane number and density (g/cm^3 , 15.6°C) of the diesel fuels were measured using the ASTM D613 and ASTM D4052 methods, respectively. Hydrocarbon type compositions of the fuels were determined by GC-FIMS and PIONA. In each sample, the material boiling in the $200 - 343^\circ\text{C}$ range was analyzed by GC-FIMS while PIONA was used to analyze the material boiling at temperatures lower than 177°C . The sum of GC-FIMS and PIONA results, weighted with the corresponding mass fractions, gave the total hydrocarbon composition of the blend. For the GC-FIMS determinations, a $30 \text{ m} \times 250\mu\text{m} \times 0.25\mu\text{m}$ HP1-MS non-bonded column was used. The injection ($0.2\mu\text{L}$; 19:1 split) was made with the oven at 45°C . The AC PIONA analyzer based on HP GC 5890 instrument was used to perform the analysis. It was operated under the 'mode 20' conditions (normal paraffins, isoparaffins, naphthenes, and aromatics). Further details are reported elsewhere¹.

A three-layer Ward backpropagation network with three hidden slabs (WSGN – NeuroShell® software, Ward System Group Inc. MD, USA) was used in neural network correlations². Including the original diesel fuels and the diesel blends, a total of 129 samples were used to construct the neural network correlations. The 129 samples were divided into three data sets: training set, test set and production set. Two steps were required to create the three-layer backpropagation neural network model: a training step and a validation step. In the training step, the neural network was supplied with the training data set, including the input and corresponding output values. The network learned the trends contained in the data

set and correlated the inputs and outputs by finding the optimum set of weights that minimized the differences between the predicted outputs and the actual outputs. The test set was used with calibration during the training process to prevent over-training of networks, such that they would generalize well on new data. During the validation step, the neural network was provided with the production data set, not seen during the training step, to compute an average error for the test set of this model. The training terminated when 20,000 epochs had passed since reaching of the minimum average error for the test data set.

Twelve hydrocarbon types were used as neural network inputs, and density or cetane number was the network output. Table 1 lists the maximum and minimum values of the inputs and outputs for all the diesel samples used in this study. As shown in the table, the diesel samples used in this work cover a wide range of chemical composition and physical properties.

Table 1. Maximum and minimum values of the neural network inputs and outputs

	Max	Min
Inputs (mass%)		
Isoparaffins	33.09	0.70
n-Paraffins	20.95	0.37
Monocycloparaffins	29.42	1.60
Dicycloparaffins	28.38	0.27
Polycycloparaffins	31.80	1.29
Alkylbenzenes	18.31	5.81
Benzocycloalkanes	31.36	3.08
Benzodicycloalkanes	10.37	0.09
Diaromatics	62.51	0.74
Triaromatics	3.92	0.00
Tetraaromatics	0.63	0.00
Aromatic sulfurs	5.07	0.01
Outputs		
Density (g/ml @ 15.6°C)	0.9569	0.7985
Cetane (CN)	58.4	18.7

Results and Discussion

The consistency of the blending process was checked by comparing the density of the diesel blends measured by ASTM D4052 with the calculated weight averaged density derived from original diesel fuels by the following equation:

$$d = \sum_{i=1}^n d_i W_i$$

where n is the number of original diesel blending components that contributed to the blend, d_i is the density of the i^{th} blending component, W_i is the weight fraction of the i^{th} component in the blend. Figure 1 plots the calculated densities of the blends versus those measured by ASTM D4052. Good agreement between the two sets of data is demonstrated there.

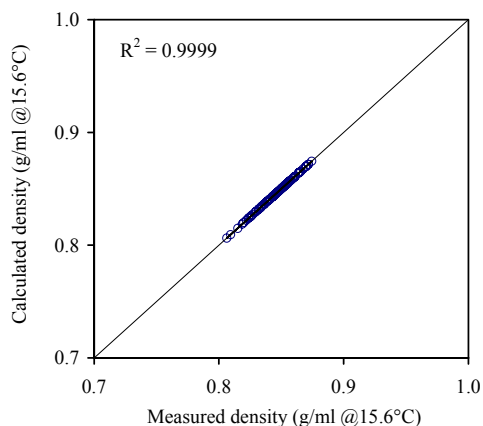


Figure 1.
Comparison of weighted average density with measured density

Density correlation

The twelve hydrocarbon types listed in Table 1 were used as inputs, and density as the output for the three-layer Ward backpropagation network. Seventy-five diesel blends were chosen as the neural network training data set. To cover the whole range of the diesel fuels in this study, the training data set included the 15 original diesel blending components that contained the maximum and minimum values of inputs and outputs. Twenty diesel blends were included in the test set and 34 diesel blends were in the production set.

The densities of all the diesel blends were calculated with the obtained neural network models. The results are plotted in Figure 2 (open circle) showing parity between the calculated and measured densities. Unfortunately, the correlation coefficient obtained was only 0.8560.

In order to improve the predictions, we carefully examined the boiling range (Simdist ASTM D2887) of the diesel blends, and found that 30 diesel blends contained substantial amount of material boiling higher than 343°C. Since the GC-FIMS method we employed could only give reliable hydrocarbon compositions in the range between 200 to 343°C, the hydrocarbon compositions of these 30 heavier diesel blends were found erroneous. A new neural network model was completed after we removed the 30 blends from the data set. The new model was used to calculate the densities of the remaining 99 diesel blends. The results were compared with the previous ones in Figure 2 (close circle). A significant improvement was achieved. A correlation coefficient of 0.9875 was obtained in this case.

Cetane number correlation

Neural network correlations for predicting cetane numbers from the diesel fuels' chemical compositions were established using both full diesel blends (129 sample data) and diesel blends without the 30 heavy samples (99 sample data). Figure 3 shows the neural network predicted versus measured cetane numbers in both cases. The results indicate that the removal of the 30 heavy diesel blends benefits the cetane number correlation.

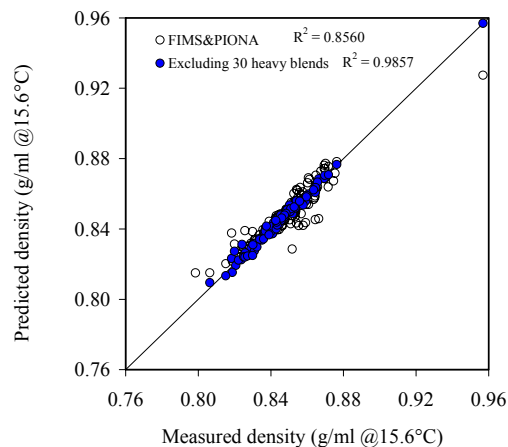


Figure 2.
Comparison of calculated density with measured density with (○) and without (●) 30 heavy diesel blends

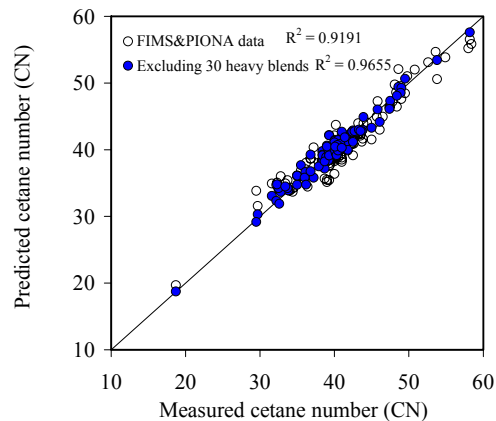


Figure 3.
Comparison of calculated cetane number with measured cetane number with (○) and without (●) 30 heavy diesel blends

NCUT had previously developed neural network correlations for densities and cetane numbers of diesel fuels from chemical compositions using the same three-layer Ward backpropagation network³. A smaller database with 69 diesel blends was used in that case. LC/GC-MS (liquid chromatography (LC)/gas chromatography-mass spectrometry) was used to determine the chemical compositions of diesel fuels. Good correlation results were obtained in our previous study. In the present work, the chemical composition was determined by the sum of PIONA and GC-FIMS. GC-FIMS has several advantages over GC-MS. In GC-FIMS the sample can be analyzed entirely without separating into saturate and aromatic fractions, which reduces the error caused by lost of lighter and heavy ends during the separation procedure. GC-FIMS can also distinguish n-paraffins from iso-paraffins, which increases the prediction accuracy of the correlations since n-paraffins and iso-paraffins have different effects on cetane number and density. The statistical results

of density and cetane number obtained in the present work and previous work are compared in Table 2.

Table 2. Comparison of the statistical results for density and cetane number predictions using neural network models derived from GC-MS and GC-FIMS +PIONA results

	Density		Cetane number	
	GC-MS	GC-FIMS	GC-MS	GC-FIMS
	PIONA		PIONA	
R-square	0.96	0.99	0.91	0.97
Mean absolute error	0.004	0.002	1.32	0.72
Max absolute error	0.009	0.007	6.9	2.85
Percentage with 5%	100	100	81.2	94.9

Two conclusions can be drawn from Table 2. First, the mean absolute error for cetane number prediction from both neural network models were below the reproducibility limits of the ASTM D613 engine test method, which was between 2.8 to 4.8 depending on the cetane number of diesel fuel. However, the mean error for the density prediction was not as good as the reproducibility of the ASTM D4052 test (0.0005). Second, the neural network correlations developed using more detailed hydrocarbon composition (sum of GC-FIMS and PIONA) as well as a larger database (the current work) resulted in substantial improvements of density and cetane number predictions over the neural network correlations developed using GC-MS and the smaller database. The mean absolute error for density decreased from 0.004 to 0.002 when the current model replaced the previous neural network model. The mean absolute error for cetane number reduced from 1.32 to 0.72 when the new model was used. These correlations could probably be further improved by introducing more inputs or slightly different inputs to the correlations. The former requires a greater experimental database but the latter could be done using the same database.

Conclusions

A neural network method was used to establish correlations for density and cetane number for a diesel fuel from its chemical composition determined by GC-FIMS and PIONA. The results show that reliability of the hydrocarbon compositions is very important to create accurate neural network correlations. Significant improvement was obtained for both density and cetane number correlation after the removal from the database of 30 heavy diesel blends that could not be characterized correctly by the GC-FIMS method. The neural network correlation could predict the cetane number with mean absolute error well below the reproducibility limit of the ASTM engine test method. However, further effort is needed to develop a better correlation for density prediction. Our results also showed that significantly better neural network correlations were obtained using hydrocarbon compositions derived from GC-FIMS + PIONA and a large database.

Acknowledgement. Partial funding for this work has been provided by the Canadian Program for Energy Research and Development (PERD), the Alberta Research Council and The Alberta Energy Research Institute. The authors wish to thank NCUT's analytical staff for all the analyses.

References

- (1) Briker, Y.; Ring, Z.; Iacchelli, A.; McLean, N.; Fairbridge, C., Malhotra, R.; Coggiola, M.; Young, S.; *Energy & Fuels*, **2001**, *15*, 996.
- (2) NeuroShell® 2 Manual. Ward Systems Groups, Inc. MD. 1996.
- (3) Yang, H.; Ring, Z.; Briker, Y.; Mclean, N.; Friesen, W.; Fairbridge, C.; *Fuel*, **2002**, *81*, 65.

Effects of Molecular Composition and Carbonization Reactivity of FCC Decant Oil and its Derivatives on Mesophase Development

Semih Eser and Guohua Wang

Department of Energy and Geo-Environmental Engineering and
Energy Institute
The Pennsylvania State University, 101 Hosler Building University
Park, PA 16802

Introduction

FCC decant oil is the primary feedstock to delayed coker to produce needle coke, a premium carbon precursor to synthetic graphite electrodes. Mesophase development during coking, determines the graphitizability of the needle coke product. Mesophase development, in turn, depends on the molecular composition of the feedstocks [1,2].

In a commercial delayed coking unit, liquid-phase carbonization (coking) takes place in insulated coke drums as the feed, heated in a tubular furnace, flows upward in the drums [3]. Liquid products from delayed coking are separated into light and heavy oils by distillation in a fractionator. Fresh feed (typically decant oil) is also fed to the fractionator. The furnace charge (coker feed) comes from the bottom of the fractionator that includes the heavy ends of both fresh feed and liquid products from coking.

Most studies on delayed coking have used FCC decant oil as the feedstock material, although the actual coker feed may have a very different composition from that of the parent decant oil. The objective of this study is to analyze the molecular composition of the coker feeds as compared to the parent decant oils. Laboratory carbonization experiments were carried out on the decant oil and coker feed samples as well as on the bottom and top fraction (gas oil) of the decant oils separated by vacuum distillation. Samples of hydrotreated gas oil were also carbonized under comparable conditions. Semi-coke and asphaltene yields from the carbonization experiments were determined to compare the carbonization reactivity of different samples. Mesophase development was monitored by polarized-light microscopy of semi-coke samples.

Experimental

The samples used for both analysis and carbonization experiments include two sets of decant oils (DO3-1 and DO3-3), coker feed (CF3-1 and CF3-3), and gas oil (GO3-1 and GO3-3). Samples of hydrotreated gas oil (HYD3-1 and HYD3-3) and vacuum tower bottoms (VTB3-1 and VTB 3-3) were used only in the carbonization experiments.

Gas Chromatography/Mass Spectrometry (GC/MS), was used to determine the concentrations of GC-amenable aromatic compounds, using a method reported elsewhere [4].

Carbonization experiments were carried out in 15 mL tubing bomb reactors under autogenous pressure at two different temperatures using a sample size of 4 g. A lower temperature (450°C) was used to determine the product yield from the carbonization of individual samples for 15 min to 180 min. Carbonization at higher temperature (500°C) for 4 – 6 h was carried out to examine the optical texture of semi-coke products to monitor mesophase development.

Semi-coke samples were prepared in epoxy resin pellets, and the polished pellets were examined using a polarized light microscope. We used a 1.1 mm X 1.1 mm mask and 10X object lens to acquire surface images. At least 150 images were examined for each sample. The extent of mesophase development that produced the semi-coke

texture was expressed in terms of an Optical Texture Index (OTI) [1] as a measure of structural anisotropy. Higher OTI, higher is the degree of anisotropy in terms of the shape and size of optical units observed under a polarized-light microscope. The desired needle coke anisotropy will consist mostly of the flow domain texture that represents elongated regions of liquid crystalline (mesophase) structures. Domains, and small domains represent a decreasing extent of anisotropy in this order.

Products from low temperature (450°C) carbonization were separated into semi-coke (dichloromethane insoluble), asphaltenes (dichloromethane soluble and pentane insoluble), and maltenes (pentane solubles) to determine the semi-coke and asphaltene yields.

Results and Discussion

Table 1 shows the OTI of semi-cokes obtained from carbonization of different samples. The two decant oil samples produced semi-cokes with very different OTI under the same experimental conditions: 83 for DO3-1 and 66 for DO3-3. A similar trend was observed when comparing the semi-coke textures for the respective derivatives (except HYD), although the differences were not as significant as that obtained with the DO samples. In contrast, HYD03-1 gave a lower value of OTI than that of HYD03-3. Within each sample set, CF produced more developed textures than the parent DO. This difference was particularly pronounced for sample Set 03-3 where CF OTI (82) is much higher than DO OTI (66), indicating a substantially improved mesophase development from CF03-3 compared to DO03-3. GO produced the worst optical texture within each sample set. GO3-1 produced a better texture than GO3-3, whereas HYD03-1 produced a worse texture than HYD03-3. This reversal in the trend of texture development suggests that hydrotreatment can very significantly change the resulting optical texture obtained from the carbonization of the hydrotreated products compared to the starting GO. VTB produced better textures than DO and CF in both sample sets. While VTB produced the most developed texture in Set 03-1 (OTI:95), HYD gave the most developed texture in Set 03-3 (OTI: 94).

Table 1. Optical Texture Indices for semi-cokes produced by carbonization at 500°C, for 4 h and 6 h (GO and HYD).

	Set 03-1	Set 03-3
DO	83	66
CF	88	82
GO	61	54
HYD	87	94
VTB	95	86

Figures 1-4 present the concentrations of polyaromatic hydrocarbons in DO, CF, and GO and n-alkanes in DO in both sample sets. It is shown in Figure 1 that DO3-1 has a higher overall pyrenes/phenathrenes (py/ph) ratio compared to DO3-3.

Figure 2 compares the n-alkanes distributions in DO samples. The DO3-3 has higher concentrations of large n-alkanes (>20 carbon atoms) than DO3-1. These differences in the composition of the aromatic compounds and n-alkanes in the two DO samples can be related to the difference observed in the semi-coke textures between DO3-1 and DO3-3 semi-cokes. It has been reported that higher py/ph ratios and lower concentrations of large alkanes in decant oils lead to higher degrees of mesophase development upon carbonization [1].

A comparison of Figure 1 and Figure 3 shows that CF samples have much higher py/ph ratios than the corresponding DO samples. Again, this difference can explain the more developed textures

obtained from CF compared to the corresponding DO. It is noted, however, that CF3-3 has a higher py/ph ratio than CF3-1, although the semi-coke texture from CF3-1 is slightly worse than CF3-3. This discrepancy may be attributed to the difference in the composition of the heavy ends that cannot be resolved by GC/MS. The fact that VTB3-1 produced a much better texture than VTB3-3 (Table 1) suggests a significant difference in the molecular composition of the heavy ends of the two samples. It should be noted that VTB constitutes a significant fraction of CF. Laser Desorption/Mass Spectrometry and High-Pressure Liquid Chromatography results indicated that five-ring aromatics (benzopyrene and benzopyrenes) are more abundant in CF and VTB [5].

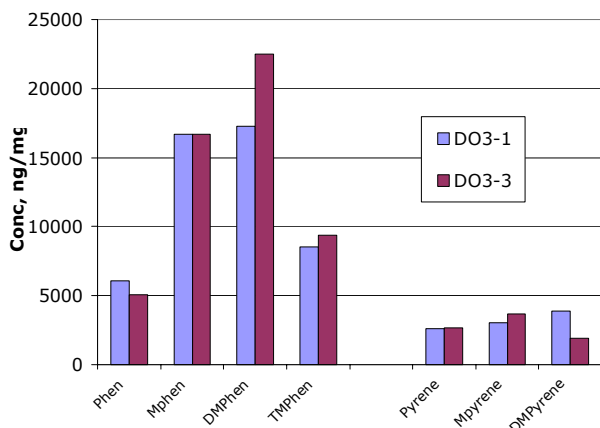


Figure 1. PAHs in decant oils (DO)

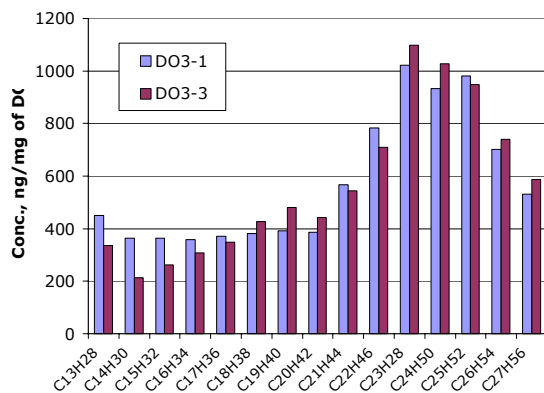


Figure 2. n-alkanes in decant oils (DO)

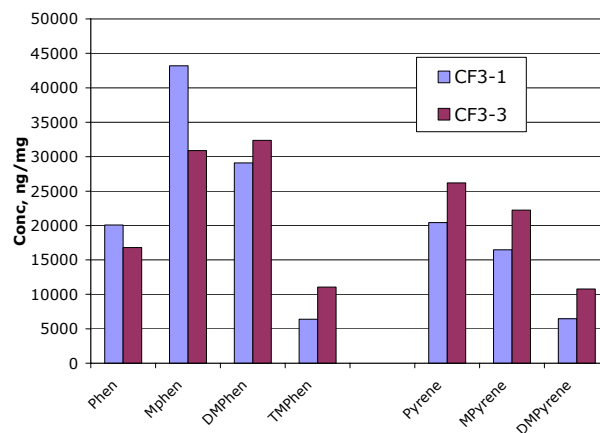


Figure 3. PAHs in Coker Feed (CF)

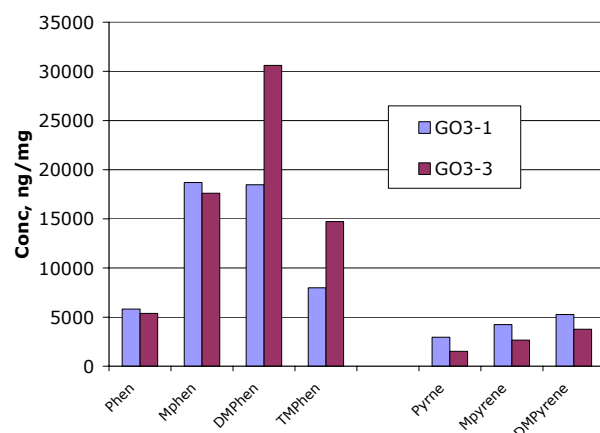


Figure 4. PAHs in Gas Oil

Figures 5-7 present the semi-coke and asphaltene yields from carbonization at 450°C. Figure 5 shows that DO3-3 has the highest semi-coke yield among the samples after relatively long reaction times (>120 min). In contrast, HYD03-3 gave the lowest semi-coke yields, as expected. A sharp increase was observed in the semi-coke yield from GO during the very early stages of carbonization between 15 and 30 minutes, CF03-3, on the other hand, showed a slow and steady increase in the semi-coke yield throughout the reaction time period. Figure 6 shows the asphaltene yields. Among the samples, CF03-3 stands out with much higher asphaltene yields than the other samples throughout the whole reaction time period. HYD03-3, on the other hand, gave the lowest asphaltene yields among the samples (with the exception of GO after 3 h). GO shows comparable asphaltene yield to those of HYD and DO during the early stages.

A comparison of coke and asphaltene yields shows that the conversion of asphaltene to semi-coke proceeds most slowly during the carbonization of CF03-3. A very rapid initial increase in asphaltene yields from CF03-3 does not translate into a rapid build-up of semi-coke yield, indicating a prolonged presence of a fluid phase that would promote mesophase development. In direct contrast, GO3-3 shows a very fast conversion of asphaltene to semi-coke during the early (<60 min) and, particularly later stages (>120 min) of carbonization. DO also shows a relatively fast formation of semi-coke from the asphaltene. GO3-3 and DO3-3

gave the least developed textures in the sample set, as shown in Table 1.

The asphaltene and semi-coke yields from VTB03-3 show a different trend from that of the other samples. A very rapid initial increase in asphaltene yield is followed by a rapid conversion of asphaltenes to semi-coke, as shown in Figure 7. Relatively well-developed mesophase from VTB03-3 despite a fast conversion of asphaltenes into semi-coke may be attributed to a favorable interaction between the evolution of volatiles and the carbonizing viscous phase (with high asphaltene contents) to form elongated anisotropic domains.

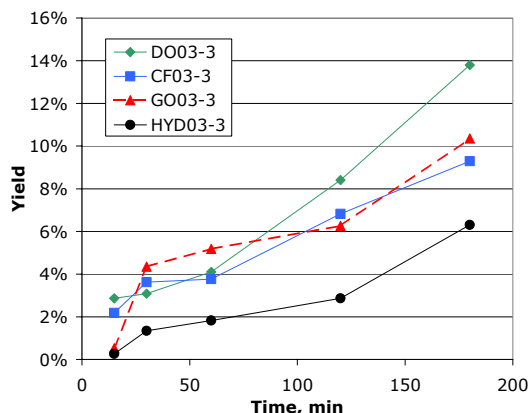


Figure 5. Coke yield at 450°C for Set 03-3.

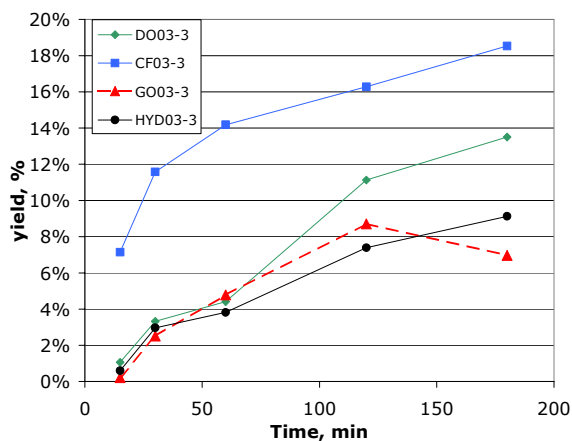


Figure 6. Asphaltene yields at 450°C for Set 03-3

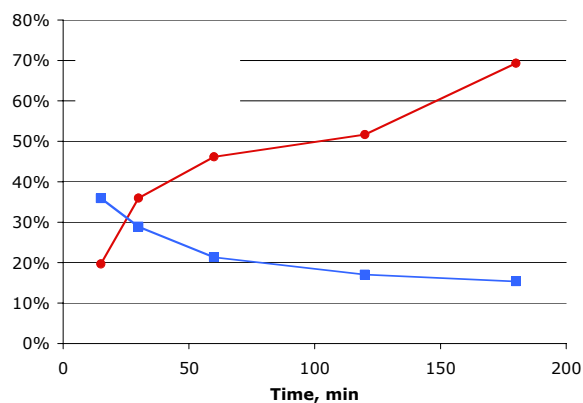


Figure 7. Coke and asphaltene yields from VTB03-3 at 450°C

Conclusions

Significant differences were observed between the molecular composition of FCC decant oil and its derivatives in two different sample sets. Coker feeds have higher concentrations of aromatic compounds and possess higher pyrenes/phenanthrenes ratios compared to the parent decant oils. Differences in the extent of mesophase development from decant oil, coker feed, gas oil, hydrotreated gas oil, and vacuum tower bottoms can be explained by differences in their molecular composition that is closely related to their carbonization reactivity. In general, slower conversion of asphaltenes into semi-coke favors a high degree of mesophase development. Conversely, at high asphaltene levels during carbonization, effective deformation of viscous anisotropic domains during conversion to semi-coke also promotes mesophase development.

Acknowledgements. We thank Carbon Research Center at Penn State and Chicago Carbon Company for their financial support. Many helpful discussions with Robert Miller of CCC are gratefully acknowledged.

References

1. Eser, S. in Supercarbon: Synthesis, Properties and Applications, ed. By Yoshimura, S. and Chang, R.P.H., Springer-Verlag, Berlin, 1998, p. 147.
2. Mochida, I., Fujimoto, K. and Oyama, T. in Chemistry and Physics of Carbon, Vol 24, ed. By Thrower, P. A., Marcel Dekker Inc., New York, 1994, p111.
3. Gary, J. H. and Handwerk, G. E., Petroleum Refining, Marcel Dekker, New York, 2001, pp. 71,72.
4. Filley, R.M. and Eser, S., Energy Fuels, 1997,11, p. 623.
5. Eser, S., Dutta, R. Wang, G. and Clemons, J., Proceedings(in CD) of International Conference on Carbon, Beijing, 2002, Keynote Presentation, Session 32.

SIMULATED DISTILLATION OF HEAVY FRACTION BY CAPILLARY SUPERCRITICAL FLUID CHROMATOGRAPHY. EVALUATION AND COMPARISON WITH GC

Laure Dahan[§], Didier Thiebaut[§], Fabrice Bertoncini*, Didier Espinat* and Alain Quignard*

§ : Ecole Supérieure de Physique et de Chimie Industrielles de Paris
10, rue Vauquelin, 75231 Paris cedex 05, France.

*: Institut français du Pétrole
IFP-Lyon -BP3-69390 Vernaison-France

Introduction

Simulated distillation (Simdis) based on gas chromatography (GC) is widely used in the petroleum industry for evaluation of fossil fuels as well as petroleum feeds and cuts treated in refining and conversion processes. Through a calibration curve relating the boiling point of normal paraffins to their elution temperature or retention time, simdis gives the hydrocarbon distribution of the sample (in weight percent) versus the boiling range of the fraction (expressed in Atmospheric Equivalent Boiling Point, AEBP). The conditions used for simdis¹ are tuned to provide results in agreement with preparative distillation that gives the True Boiling Point (TBP) curve (described in ASTM D2892). Several methods have been standardized (ASTM D2887, D5307) for samples with a final boiling point (FBP) up to 538 °C (1000 °F). Much effort has gone into extending the range of eluted compounds and the standardization of a method up to an FBP of 700 °C is in progress (ASTM proposed test method, 1994). However, at oven temperatures up to 430 °C in high-temperature GC, the resistance of high molecular-weight hydrocarbons (HMHS) to cracking reactions is questionable^{2,3,4}. This is not the case in supercritical-fluid chromatography (SFC) as high temperatures are not needed and the mechanism for extending the upper limit depends on sample solubility not volatility. Indeed, the main advantage of SFC over GC techniques comes from the solvent strength of the mobile phase. The polarity of the most commonly used supercritical mobile-phase, CO₂, depending on the operating conditions, varies between that of pentane and toluene, making SFC a potentially powerful technique for the elution of HMH at much lower temperatures than GC. This communication presents recent advances in Simdis of heavy fractions using SFC. Compared to GC, SFC calibration range is extended up to C₁₂₀ hydrocarbons and can be extrapolated to nC₁₆₂. As in GC, using element selective detectors SFC could be the tool of choice for better quantitation of conversion in heavy petroleum-fraction processing.

Experimental

Samples. The samples of feed and effluents of hydrotreatment units were obtained from IFP pilot plants. The so-called feed A is a vacuum residue having the following properties: viscosity (100°C) = 1000 cst; density 15/4 = 1.028; % weigh eluted at FBP (D 2887) = 48 % w/w. The effluents were obtained after demetallization (HDM) and after HDM and desulfurization (HDS) unit. Polyethylene standard like Polywax 650 and 1000 were also used to generate retention time versus boiling point calibration.

Characterization Method. An ISCO 100D supercritical fluid syringe pump equipped with specific cooling device was used. The chromatographic column was placed into a HP 6890 gas chromatograph equipped with a flame ionization detector and coupled to G 2350 A atomic emission (Agilent technologies). Splitless injections were done using a Valco Valve CI4WE1 using 1200 nl loop at 120°C after dilution into xylene for dissolving samples³. A (5 m x 0.05 mm x 0.2 µm) capillary column DB-5 from JW was used as stationary phase. GC simdis was performed upon the

ASTM standard method (ASTM D2887, D5307 and ASTM proposed test method for HT-GC, 1994)⁴ for samples with a FBP up to 538 °C and 700 °C, respectively. The SFC system is described in **Figure 1**.

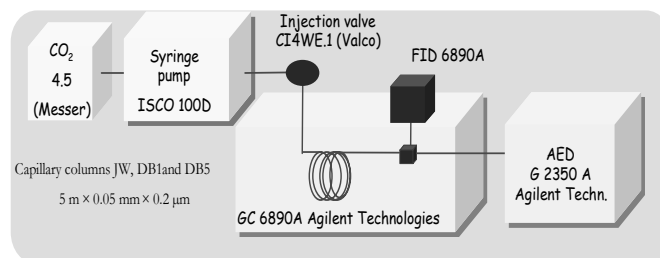


Figure 1. SFC-AED-FID hyphenation

Results and discussion

SFC simdis. Operating conditions (type stationary phase, oven temperature and pressure gradient, injection) were optimized to obtain true relationship between retention and boiling point and to avoid discrimination of sample during the injection step. Besides, it has been necessary to obtain the lowest difference between the retention of different compounds having the same boiling point (e.g. alkanes and aromatics) for better accuracy of distillation curves. Polydimethylsiloxane bounded phases were carried out to provide no selectivity versus structure^{3,5}. Thanks to optimisation of phase ratio, the heaviest compound eluted was n-C₁₁₈, what was quite higher than previously reported (C₁₀₈)⁵. An example of chromatogram of standard mixture is given on **Figure 2**.

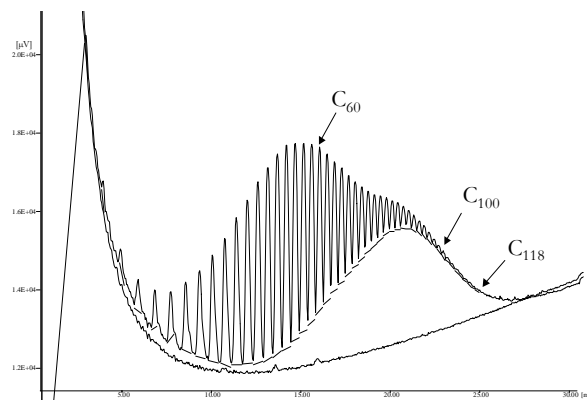


Figure 2. Chromatogram of polywax 655/1000 mixture (50/50 w/w). Conditions: Column DB5 (5 m x 0,05 mm x 0,2 µm); 6.6 g/L; Flow-rate (CO₂) = 3 ml / min; T_{oven} = 160°C; Pressure (CO₂) 100 bars to 500 bars (30 min) at 13.3 bars/min.

Routine detection of n-C₁₂₀ (750 °C) was observed, what means a benefit of 20 carbons benefit with regard to HT- GC (e.g. end point benefit of 50 °C). Repeatability was daily checked as critical for simdis: 20 injections of a test mixture over 35 days lead to retention time RSD less than 0.3%.

Model of retention vs. number of carbon atoms in SFC. Owing to the lack of resolution, it was not possible to identify elution peaks at the end of the chromatogram of Polywax 1000. In order to calibrate this part of the chromatogram, a model calculating n-paraffins retention times between C₅₀ and C₁₀₀ as a function of their

number of carbon atoms has been implemented. This model has been performed to check for retention time of n- paraffins in the range of C_{100} to C_{120} , for whom retention times were known from the chromatogram, and to predict retention times in the range of C_{120} to C_{162} . The comparison between calculated and measured retention times for the identified alkanes over C_{100} lead to a bias lower than 0.07 minute. The extrapolated retention times have been used to generate simulated distillation curves from C_{26} (412 °C) to C_{162} (817 °C). The **Figure 3** shows measured retention times (from C_{26} to C_{118}) and extrapolated retention times (from C_{100} to C_{162})

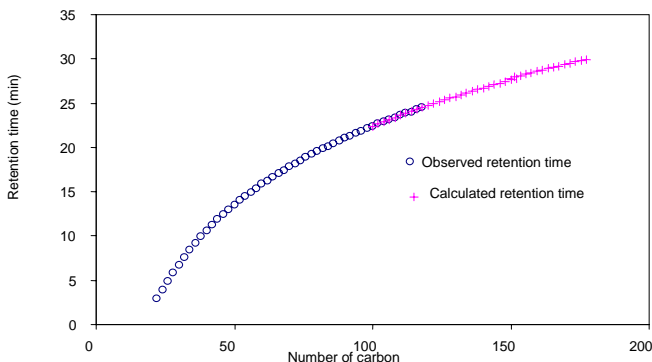


Figure 3. Comparison of extrapolated and measured retention times.

This model was carried out to characterize heavy ends using *extended SFC simdis*.

Application to feed and cuts of hydroconversion units. Our system was carried out to characterize feed A (vacuum residue) for hydroconversion unit. **Figure 4** shows the chromatogram and the upper boiling point limit typically obtained using HT-GC (nC_{106} , 731°C) and extended SFC (nC_{162} , 817°C) are indicated on the chromatogram.

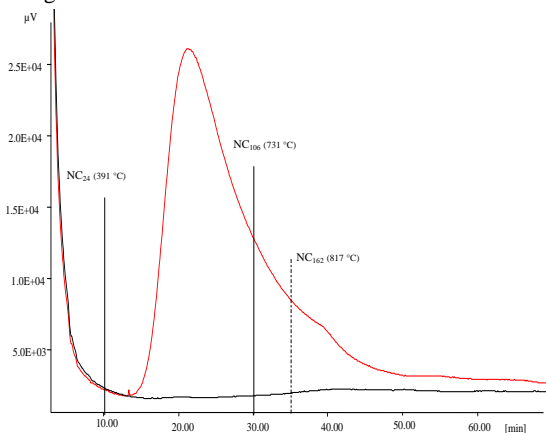


Figure 4. Chromatogram of A feed (vacuum residue)

Conditions: Column DB5 (5 m × 0,05 mm × 0,2 µm); 100 g/L; Flow-rate (CO_2) = 2 ml/min; T_{oven} = 160°C; Pressure (CO_2) 100 bars (5 min) to 550 bars (30 min) at 13.3 bars/min.

Clearly, the ability of SFC to provide the elution of HMW enables a better representation of the feed: the FBP according to HT-GC simdis corresponds to 74 % w/w of eluted fraction using SFC, what is quite less than 85 % w/w of the eluted fraction at FBP using extended SFC simdis. **Figure 5** shows simulated distillation curves obtained for HT-GC, SFC and extended SFC.

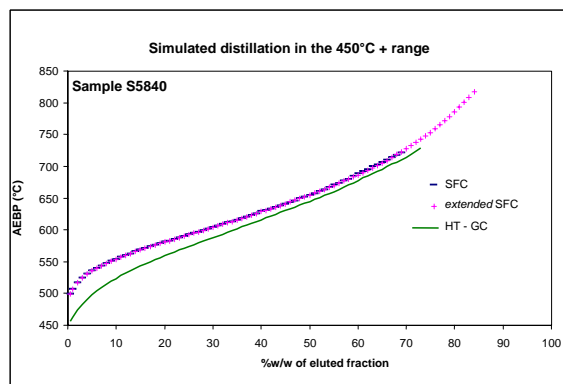


Figure 5. Comparison of simdis curves using HT-GC, SFC and extended SFC.

It is obvious that good agreement is observed between the GC and SFC data in the range of 450 °C to 731°C, as previously reported^{3,5}. Using extended SFC, the upper limit can be raised above 810 °C, enabling approximately 90% of this heavy residue to be characterized. **Table 1** reports the weight percent of eluted fraction corresponding at several boiling points and different samples.

Table 1 : weight percent of eluted fraction for feed and effluents obtained using extended SFC.

Boiling point (°C)	Feed A (vacuum residue) % w/w	Effluent HDM % w/w	Effluent HDM - HDS % w/w
500	0.58	0.57	4.98
600	28.3	39.72	11.07
700	63.66	70.54	51.39
750	74.39	78.89	78.53
800	81.91	84.52	88.5

As opposite to the GC simdis, SFC simdis extends the range of this application up to nC_{162} , providing better quantitation of conversion in heavy petroleum-fraction processing.

Conclusions

SFC is well adapted to the characterization of heavy hydrocarbons because of the solvating properties of supercritical fluids and could be applied in routine simulated distillation for extending the range of the technique. Besides, work is on progress to take benefit from detection facilities of SFC to perform specific Simdis curves.

References

- 1) Peaden, P. A. *J. High Resol. Chromatogr.* **1994**, 17, 203.
- 2) Schwartz, M. M.; Brownlee, H. E.; Boduszynski, R. G.; Su, F. *Anal. Chem.* **1987**, 59, 1393.
- 3) Roberts, I. *Supercritical-fluid chromatography*, in Adlard, E. R., Ed., *Chromatography in the Petroleum Industry*, Elsevier, NL, 1995, Chap.11..
- 4) Durand, J. P.; Bré, A.; Béboulène, J. J., Ducrozet, A., Carbonneaux, S. *19th Int. Symp. on Capillary Chromatography and Electrophoresis*, Wintergreen, May **1997**.
- 5) Robert, E.; in Caude, M.; Thiebaut, D.; Ed "*Supercritical fluid chromatography and extraction*", Harwood Academic Publishers, amsterdam,1999, chap.9..